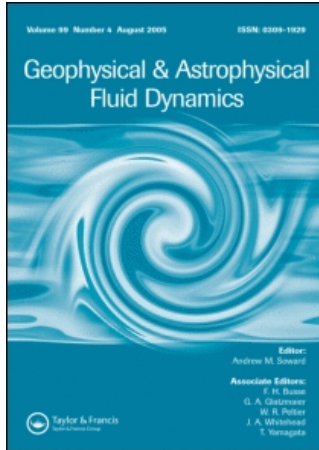


This article was downloaded by:[Soward, Andrew]  
On: 5 March 2008  
Access Details: [subscription number 772390772]  
Publisher: Taylor & Francis  
Informa Ltd Registered in England and Wales Registered Number: 1072954  
Registered office: Mortimer House, 37-41 Mortimer Street, London W1T 3JH, UK



## Geophysical & Astrophysical Fluid Dynamics

Publication details, including instructions for authors and subscription information:  
<http://www.informaworld.com/smpp/title-content=t713642804>

### The instability of precessing flow

R. R. Kerswell<sup>a</sup>

<sup>a</sup> Department of Mathematics and Statistics, University of Newcastle upon Tyne, England, UK

Online Publication Date: 01 November 1993

To cite this Article: Kerswell, R. R. (1993) 'The instability of precessing flow',  
Geophysical & Astrophysical Fluid Dynamics, 72:1, 107 - 144

To link to this article: DOI: 10.1080/03091929308203609

URL: <http://dx.doi.org/10.1080/03091929308203609>

PLEASE SCROLL DOWN FOR ARTICLE

Full terms and conditions of use: <http://www.informaworld.com/terms-and-conditions-of-access.pdf>

This article maybe used for research, teaching and private study purposes. Any substantial or systematic reproduction, re-distribution, re-selling, loan or sub-licensing, systematic supply or distribution in any form to anyone is expressly forbidden.

The publisher does not give any warranty express or implied or make any representation that the contents will be complete or accurate or up to date. The accuracy of any instructions, formulae and drug doses should be independently verified with primary sources. The publisher shall not be liable for any loss, actions, claims, proceedings, demand or costs or damages whatsoever or howsoever caused arising directly or indirectly in connection with or arising out of the use of this material.

# THE INSTABILITY OF PRECESSING FLOW

R. R. KERSWELL

*Department of Mathematics and Statistics, University of Newcastle upon Tyne,  
NE1 7RU, England, UK*

*(Received 16 November 1992; in final form 22 March 1993)*

An explanation is put forward for the instability observed within a precessing, rotating spheroidal container. The constant vorticity solution for the flow suggested by Poincaré is found to be inertially unstable through the parametric coupling of two inertial waves by the underlying constant strain field. Such resonant couplings are due either to the elliptical or shearing strains present which elliptically distort the circular streamlines and shear their centres respectively. For the precessing Earth's outer core, the shearing of the streamlines and the ensuing shearing instability are the dominant features. The instability of some exact, linear solutions for finite precessional rates is established and used to corroborate the asymptotic analysis. A complementary unbounded analysis of a precessing, rotating fluid is also presented and used to deduce a likely upperbound on the growth rate of a small disturbance. Connection is made with past experimental studies.

**KEY WORDS:** Precession, Earth's core, inertial waves, rotating fluids

## INTRODUCTION

The problem of understanding the fluid motion within a precessing spheroidal cavity has received considerable attention over the years, motivated initially by its relevance to astrophysical and geophysical contexts, and sustained by the wealth of interesting phenomena revealed by laboratory experiments (Malkus 1968, and more recently Vanyo 1991; Vanyo *et al.* 1992). Despite the simple geometry and the small number of parameters which enter into the physical description, Malkus found that the flow possessed some unusual properties including the possibility of a fully disordered state. An outstanding issue for geodynamicists then became whether this laboratory picture of a disordered flow was more relevant to the precessing Earth's outer core than Poincaré's (1910) elegant laminar solution.

In an attempt to rationalise the experimental findings, past work has concentrated exclusively upon viscous effects. After the initial work of Bondi and Lyttleton (1953), Stewartson and Roberts (1963, 1965) established that Poincaré's (1910) elegant constant-vorticity solution for a precessing, oblate spheroid is realised and may be corrected to account for viscosity by the addition of a thin Ekman layer on the container walls. Following on from this in a paper which seemed to reach as far as was analytically viable, Busse (1968) deduced that a nonlinear, viscous boundary layer would induce a small differential rotation upon Poincaré's solution. This differential rotation was localised around the cylindrical shear layer (connecting the known

boundary layer eruptions at  $\pm 30^\circ$  latitude relative to the equator defined by the bulk flow vorticity) and was confirmed by Malkus' dye streak experiments. At this point, the observed instability was interpreted as the local breakdown of this shear layer.

In this paper, we offer an alternative explanation for the observed instability by demonstrating that Poincaré's solution is, in fact, inertially unstable. A cursory glance at the form of Poincaré's solution does not warn of instability; it appears a simple, laminar flow in which the vorticity is spatially and temporally constant in the precessing frame and displaced from the container's axis. A closer inspection reveals that the flow actually suffers a constant straining throughout its bulk and it is this which may cause the flow to bifurcate at sufficient speeds of precession.

The mechanism of instability is similar to that which underlies the elliptical instability (Gledzer *et al.*, 1975; Vladimirov and Tarasov, 1984; Vladimirov and Vostretsov, 1986; Waleffe, 1989; Malkus, 1989; Kerswell, 1993a, b) as conjectured recently by Malkus (1993); two inertial Poincaré modes of the system are resonantly coupled by the underlying strained state. The straining field produced within a precessing spheroid consists of an 'elliptical' component in the plane of the streamlines and a 'shearing' component perpendicular to this plane so that the streamlines are elliptically-distorted and sheared. However, although the elliptical strain is present it is not the primary consequence of precession but rather a secondary, boundary-induced effect. Instead, the generic feature of precessional flows appears to be the shearing of the streamlines, apparent from the unbounded analysis. This realisation, along with its implications for stability, represents the main conclusion of this work. Certainly for Earth-like parameters, it is the shearing strain which is by far the most significant feature of a Poincaré-like solution in the outer core.

The only previous work to consider the excitation of inertial waves in a precessing spheroid is due to Greenspan (1968, p 68) who treated the problem as that of forced motion upon uniform rotation due to the time variation of the total angular velocity. Consequently, a resonant response was only anticipated (to lowest order) when the forcing frequency coincided with an inertial wave frequency. Armed with Poincaré's basic state, we treat the problem as one of bifurcation and find that resonant growth of two inertial waves can occur when the *difference* in their frequencies coincides with one of the 'distortion' frequencies of the basic flow (the ellipticity and shearing of the basic streamlines give 'distortion' frequencies of  $2\Omega$  and  $\Omega$  respectively where  $\Omega$  is the container's angular velocity). The absence of any basic solution in a precessing, rotating cylinder means that the problem can only be treated from the forced standpoint (see Johnson, 1967; Gans, 1970; Thompson, 1970 and Manasseh, 1992). This said, in a concurrent, independent study, Mahalov (1992) has considered an infinite cylinder in which a tilted (sheared) streamline solution can exist under precession. His findings appear consistent with the conclusions of this paper.

Once bounded inertial waves are excited, many studies have documented how they tend to dramatically breakdown or collapse to a disordered or turbulent state (see for example Johnson, 1967; McEwan, 1970 who coined the term resonant collapse, Thompson, 1970; Gledzer *et al.*, 1974; Scott, 1975; Whiting, 1981; Stergiopoulos and Aldridge, 1982; Vladimirov *et al.*, 1987; Malkus, 1989 and Manasseh, 1992). While an explanation for this phenomena is beyond the scope of this paper, it seems that the

disordered state observed by Malkus (1968) in his precessional experiments is yet another manifestation of this process.

The study of rotating masses of fluid has a long and fascinating history, discussed most notably by Lamb (1932, chapter XII), Lyttleton (1953) and Chandrasekhar (1969). Although the emphasis has been to consider self-gravitating systems, there is much in common with the study of contained rotating fluids. In particular, spatially-constant vorticity disturbances were a very common tool used to diagnose instability of equilibrium configurations. In the same spirit, we construct exact linear disturbances, valid for arbitrary precession rates, to determine sufficient conditions for instability. These disturbances, of which the constant-vorticity solution is but the simplest, can be constructed from finite, closed subsets of the inertial waves of the system. Such a technique may be used to examine the stability of any linear, possibly time-dependent, basic flow inside a rotating, spheroidal container.

The paper is organised as follows. In Section 1, we examine Poincaré's solution for a precessing spheroid and derive the set of equations which form the basis for the subsequent asymptotic analysis. Section 2 demonstrates how a pair of free inertial modes may be resonantly excited through the underlying shearing strain. This is illustrated for some particular geometries, before the equivalent elliptical coupling analysis is sketched in Section 3. Some exact linear solutions for finite precessional rates are presented in Section 4, providing an independent demonstration of instability and allowing connection with the asymptotics. The key result underlying the construction of these exact linear disturbances is proved in Appendix A. Section 5 contains an alternative unbounded formulation of the problem. Here, following the experience of the elliptical instability, we consider the dominant shearing strain produced by precession in an unbounded domain. This acts to confirm the bounded domain analysis and allows a likely upperbound on the growth rate to be isolated. Section 6 is reserved for discussion.

## 1. FORMULATION

Poincaré's (1910) simple solution for the response of a rotating fluid to the precession of its container is

$$\mathbf{u} = \boldsymbol{\omega} \times \mathbf{r} + \nabla A$$

with respect to the precessing frame rotating at  $\boldsymbol{\Omega}$ . Here

$$\boldsymbol{\omega} = \hat{\mathbf{z}} - \frac{2 + \eta}{\eta + 2(1 + \eta)\boldsymbol{\Omega} \cdot \hat{\mathbf{z}}} \hat{\mathbf{z}} \times (\hat{\mathbf{z}} \times \boldsymbol{\Omega})$$

so that the basic rotation of the fluid is  $\hat{\mathbf{z}}$  and

$$A = \frac{\eta}{\eta + 2(1 + \eta)\boldsymbol{\Omega} \cdot \hat{\mathbf{z}}} (\boldsymbol{\Omega} \times \hat{\mathbf{z}} \cdot \mathbf{r})(\hat{\mathbf{z}} \cdot \mathbf{r})$$

in the spheroidal container  $|\mathbf{r}|^2 + \eta(\hat{\mathbf{z}} \cdot \mathbf{r})^2 = 1$ , i.e. the container's equatorial radius and rotation rate nondimensionalize the problem. This solution represents an exact, nonlinear, viscous solution for all but a thin boundary layer at the container walls necessary to satisfy the conditions on the tangential velocity. As our interest is in the inertial aspects of this flow, we will ignore the presence of the corrective viscous boundary layer. The flow is two-dimensional in planes inclined at

$$\tan^{-1} \frac{2|\boldsymbol{\Omega} \times \hat{\mathbf{z}}|}{\eta + 2(1 + \eta)\boldsymbol{\Omega} \cdot \hat{\mathbf{z}}}$$

to the container's equator, which due to the oblateness  $\eta$  gives rise to two effects. Firstly the streamlines are elliptical with a major-minor axes ratio of  $\sqrt{(1 + \beta)/(1 - \beta)}$  where

$$\beta = \frac{2\eta|\boldsymbol{\Omega} \times \hat{\mathbf{z}}|^2}{[\eta + 2(1 + \eta)\boldsymbol{\Omega} \cdot \hat{\mathbf{z}}]^2 + 2(2 + \eta)(\boldsymbol{\Omega} \times \hat{\mathbf{z}})^2},$$

and secondly the line joining the centres of these streamlines is not perpendicular to their plane but rather inclined at an angle

$$\tan^{-1} \frac{2\eta[\eta + 2(1 + \eta)\boldsymbol{\Omega} \cdot \hat{\mathbf{z}}]|\boldsymbol{\Omega} \times \hat{\mathbf{z}}|}{[\eta + 2(1 + \eta)\boldsymbol{\Omega} \cdot \hat{\mathbf{z}}]^2 + 4(1 + \eta)(\boldsymbol{\Omega} \times \hat{\mathbf{z}})^2}$$

to this perpendicular. These features represent different strainings of the underlying rotation and both give rise separately to inertial instability. The instability of elliptical streamlines is now well known (e.g. Pierrehumbert, 1986; Bayly, 1986; Craik, 1989 and a more recent review in 1991; Malkus, 1989; Waleffe, 1989, 1990, and Gledzer and Ponomarev 1992 who review the Russian literature) and operates via vortex stretching in the plane of motion due to the imposed strain field. The strain which shears the streamlines in a direction perpendicular to their plane has not been discussed before but is by far the more potent influence in the precessing Earth's outer core.

To examine the flow field more closely, we enter the precessing frame where the  $z$ -axis is chosen to coincide with the axis of the container and the  $x$  direction taken such that the precessional vector may be written as

$$\boldsymbol{\Omega} = [\Omega_1, 0, \Omega_3]^T.$$

where the superscript  $T$  denotes transpose. In a new coordinate system formed by rotation of the  $x - z$  plane through

$$\tan^{-1} \frac{2\hat{\mathbf{y}} \cdot \boldsymbol{\Omega} \times \hat{\mathbf{z}}}{\eta + 2(1 + \eta)\boldsymbol{\Omega} \cdot \hat{\mathbf{z}}}$$

about the  $y$ -axis, the velocity is

$$\mathbf{u} = \frac{1}{2\sqrt{1+\mu^2}} \begin{bmatrix} 0 & -[2+(2+\eta)\mu^2] + \eta\mu^2 & 0 \\ [2+(2+\eta)\mu^2] + \eta\mu^2 & 0 & -2\eta\mu \\ 0 & 0 & 0 \end{bmatrix} \mathbf{x}, \quad (1.1)$$

and the precession vector is transformed to

$$\boldsymbol{\Omega}^* = [\Omega_1^*, 0, \Omega_2^*]^T = (1+\mu^2)^{-1/2} [\Omega_1 - \mu\Omega_3, 0, \mu\Omega_1 + \Omega_3]^T \quad (1.2a)$$

with

$$\mu = \frac{2\Omega_1}{\eta + 2(1+\eta)\Omega_3}. \quad (1.2b)$$

The resultant streamlines are ellipses with sheared centres,

$$\left(x - \frac{2\varepsilon}{1+\beta}z\right)^2 + \left(\frac{1-\beta}{1+\beta}\right)y^2 = \text{const.}, \quad (1.3)$$

where

$$\varepsilon = \frac{\eta\mu}{2+(2+\eta)\mu^2} \quad \text{and} \quad \beta = \frac{\eta\mu^2}{2+(2+\eta)\mu^2}$$

measure the shearing of the streamlines and the elliptical distortion of the streamlines respectively. Their relative magnitude depends on the precessional vector  $\boldsymbol{\Omega}$  via

$$\frac{\beta}{\varepsilon} = \mu = \frac{2\Omega_1}{\eta + 2(1+\eta)\Omega_3}. \quad (1.4)$$

and for the Earth,  $\mu \sim 1.6 \times 10^{-5}$ ; the shearing of the streamlines is much the dominant effect.

Consideration of the linear stability of the flow (1.1) is hampered by its lack of symmetry; the flow is neither axisymmetric nor invariant in the direction perpendicular to its plane. Furthermore, the  $z$ -axis of our new coordinates no longer coincides with the container's axis of symmetry leading to an awkward boundary description. One possibility is to reconsider the flow back in the original container coordinates. This certainly restores the boundary to a manageable form but hides the underlying structure of the basic flow. Progress is only viable for small  $\mu$  and even then is unclear. In effect, we are forced to apply a perturbation expansion about the wrong basic state in this coordinate frame.

A less obvious but better alternative is to apply the non-orthogonal transformation

$$\begin{aligned}x &= s\sqrt{1-\beta}\cos\phi + \frac{2\varepsilon}{1+\beta}\bar{z}, \\y &= s\sqrt{1+\beta}\sin\phi, \\z &= \bar{z},\end{aligned}\tag{1.5}$$

which exploits the structure of the basic solution. This transformation serves to stretch the elliptical streamlines back into circles and then to shear them into line. The boundary is simultaneously converted back into a tractable, axisymmetric form due to its definition by an envelope of streamlines. The relevance of the first part of this transformation to elliptical flow was realised by Bayly and subsequently used to consider elliptically-distorted cylinders (Waleffe, 1989) and spheroids (Kerswell, 1993b). The new feature is the shearing transformation which slides the circles back into line. In this  $(s, \phi, \bar{z})$  coordinate system, the new velocity components  $u, v$  and  $w$  are defined such that

$$\mathbf{u} = u_x \hat{\mathbf{x}} + u_y \hat{\mathbf{y}} + u_z \hat{\mathbf{z}} = u\tilde{\mathbf{s}} + v\tilde{\boldsymbol{\phi}} + w\tilde{\mathbf{z}}$$

where the base vectors

$$\begin{aligned}\tilde{\mathbf{s}} &= \sqrt{1-\beta}\cos\phi\hat{\mathbf{x}} + \sqrt{1+\beta}\sin\phi\hat{\mathbf{y}}, \\ \tilde{\boldsymbol{\phi}} &= -\sqrt{1-\beta}\sin\phi\hat{\mathbf{x}} + \sqrt{1+\beta}\cos\phi\hat{\mathbf{y}}, \\ \tilde{\mathbf{z}} &= \frac{2\varepsilon}{1+\beta}\hat{\mathbf{x}} + \hat{\mathbf{z}}\end{aligned}$$

are neither orthogonal nor of unit length. The basic flow is now *by design* one of uniform rotation in the  $(s, \phi, \bar{z})$  system,

$$\mathbf{u} = \frac{2+(2+\eta)\mu^2}{2\sqrt{1+\mu^2}}s\tilde{\boldsymbol{\phi}} = \bar{\Omega}s\tilde{\boldsymbol{\phi}}\tag{1.6}$$

where this defines the new rotation rate  $\bar{\Omega}$ . The price paid for this simplification is the new form of the momentum equation, found by projecting onto three  $\tilde{\mathbf{l}}, \tilde{\mathbf{m}}$  and  $\hat{\mathbf{n}}$ ,

$$\begin{aligned}\tilde{\mathbf{l}} &= \frac{\cos\phi}{\sqrt{1-\beta}}\hat{\mathbf{x}} + \frac{\sin\phi}{\sqrt{1+\beta}}\hat{\mathbf{y}} - \frac{2\varepsilon\cos\phi}{(1+\beta)\sqrt{1-\beta}}\hat{\mathbf{z}}, \\ \tilde{\mathbf{m}} &= -\frac{\sin\phi}{\sqrt{1-\beta}}\hat{\mathbf{x}} + \frac{\cos\phi}{\sqrt{1+\beta}}\hat{\mathbf{y}} + \frac{2\varepsilon\sin\phi}{(1+\beta)\sqrt{1-\beta}}\hat{\mathbf{z}}, \\ \hat{\mathbf{n}} &= \hat{\mathbf{z}},\end{aligned}$$

chosen, for example, such that  $\tilde{\mathbf{l}} \cdot \tilde{\mathbf{s}} = 1$  and  $\tilde{\mathbf{l}} \cdot \tilde{\boldsymbol{\phi}} = \tilde{\mathbf{l}} \cdot \tilde{\mathbf{z}} = 0$ . The three components are exactly

$$\begin{aligned} \frac{\partial u}{\partial t} + (\mathbf{u} \cdot \nabla) u - \frac{v^2}{s} - 2 \left( \frac{\Omega_3^* + \Omega_1^* \varepsilon}{\sqrt{1 - \beta^2}} \right) v + \frac{1}{(1 - \beta^2)} \left[ 1 + \frac{2\varepsilon^2}{1 + \beta} \right] \frac{\partial p}{\partial s} \\ = \frac{2\varepsilon \cos \phi}{\sqrt{1 + \beta} \sqrt{1 - \beta^2}} \frac{\partial p}{\partial \bar{z}} + \frac{2 \sin \phi}{\sqrt{1 + \beta}} \left( \Omega_1^* - \frac{2\Omega_3^* \varepsilon}{\sqrt{1 + \beta}} \right) w \\ + \cos 2\phi \left\{ \frac{2(\Omega_1^* \varepsilon + \Omega_3^* \beta)}{\sqrt{1 - \beta^2}} v - \frac{1}{(1 - \beta^2)} \left[ \beta + \frac{2\varepsilon^2}{1 + \beta} \right] \frac{\partial p}{\partial s} \right\} \\ + \sin 2\phi \left\{ \frac{2(\Omega_1^* \varepsilon + \Omega_3^* \beta)}{\sqrt{1 - \beta^2}} u + \frac{1}{(1 - \beta^2)} \left[ \beta + \frac{2\varepsilon^2}{1 + \beta} \right] \frac{1}{s} \frac{\partial p}{\partial \phi} \right\}, \end{aligned} \quad (1.7)$$

$$\begin{aligned} \frac{\partial v}{\partial t} + (\mathbf{u} \cdot \nabla) v + \frac{uv}{s} + 2 \left( \frac{\Omega_3^* + \Omega_1^* \varepsilon}{\sqrt{1 - \beta^2}} \right) u + \frac{1}{(1 - \beta^2)} \left[ 1 + \frac{2\varepsilon^2}{1 + \beta} \right] \frac{1}{s} \frac{\partial p}{\partial \phi} \\ = - \frac{2\varepsilon \sin \phi}{\sqrt{1 + \beta} \sqrt{1 - \beta^2}} \frac{\partial p}{\partial \bar{z}} + \frac{2 \cos \phi}{\sqrt{1 + \beta}} \left( \Omega_1^* - \frac{2\Omega_3^* \varepsilon}{1 + \beta} \right) w \\ + \cos 2\phi \left\{ \frac{2(\Omega_1^* \varepsilon + \Omega_3^* \beta)}{\sqrt{1 - \beta^2}} u + \frac{1}{(1 - \beta^2)} \left[ \beta + \frac{2\varepsilon^2}{1 + \beta} \right] \frac{1}{s} \frac{\partial p}{\partial \phi} \right\} \\ + \sin 2\phi \left\{ - \frac{2(\Omega_1^* \varepsilon + \Omega_3^* \beta)}{\sqrt{1 - \beta^2}} v + \frac{1}{(1 - \beta^2)} \left[ \beta + \frac{2\varepsilon^2}{1 + \beta} \right] \frac{\partial p}{\partial s} \right\}, \end{aligned} \quad (1.8)$$

$$\begin{aligned} \frac{\partial w}{\partial t} + (\mathbf{u} \cdot \nabla) w + \frac{\partial p}{\partial \bar{z}} = - \sin \phi \left[ \frac{2\varepsilon}{\sqrt{1 + \beta} \sqrt{1 - \beta^2}} \frac{1}{s} \frac{\partial p}{\partial \phi} + 2\Omega_1^* \sqrt{1 + \beta} u \right] \\ + \cos \phi \left[ \frac{2\varepsilon}{\sqrt{1 + \beta} \sqrt{1 - \beta^2}} \frac{\partial p}{\partial s} - 2\Omega_1^* \sqrt{1 + \beta} v \right]. \end{aligned} \quad (1.9)$$

Of note here is the invariance of the advective derivative  $\mathbf{u} \cdot \nabla$  and the incompressibility condition  $\nabla \cdot \mathbf{u} = 0$ . Additionally, the form of the boundary condition remains

$$\mathbf{u} \cdot \hat{\mathbf{n}}|_{\partial V} = 0$$

with the boundary returned to its original axisymmetric form except for some rescaling, most notably of the oblateness;  $\partial V$  is

$$s^2 + (1 + \eta) \frac{(1 + \mu^2) [1 + (1 + \frac{1}{2}\eta)\mu^2]}{[1 + (1 + \eta)\mu^2]^2} \bar{z}^2 = \frac{1 + (1 + \frac{1}{2}\eta)\mu^2}{1 + (1 + \eta)\mu^2}. \quad (1.10)$$



To condense the notation a little, we introduce the vector operator

$$\mathcal{L} = \mathcal{L}(s, \phi, \bar{z}, u, v, w, p, \varepsilon, \beta)$$

whose 3 components are precisely the right-hand sides of equations (1.7), (1.8) and (1.9). We consider small disturbances  $\mathbf{u}$  upon the basic state  $\mathbf{U} = \bar{\Omega}s\bar{\phi}$  in a frame rotating with this flow. The system may now be written

$$\begin{aligned} \frac{\partial \mathbf{u}^*}{\partial t^*} + 2 \begin{bmatrix} -v^* \\ u^* \\ 0 \end{bmatrix} + \begin{bmatrix} \partial p^*/\partial s^* \\ 1/s \partial p^*/\partial \phi^* \\ \partial p^*/\partial z^* \end{bmatrix} \\ = \frac{1}{\chi} \begin{bmatrix} 1 & 0 & 0 \\ 0 & 1 & 0 \\ 0 & 0 & \alpha \end{bmatrix} \mathcal{L} \left( s^*, \phi^* + \frac{\bar{\Omega}}{\chi} t^*, \frac{z^*}{\alpha}, u^*, v^*, \frac{w^*}{\alpha}, \frac{\chi}{\alpha^2} p^*, \varepsilon, \beta \right) \end{aligned} \quad (1.11)$$

where

$$\chi = \bar{\Omega} + \frac{\Omega_3^* + \varepsilon \Omega_1^*}{\sqrt{1 - \beta^2}} = 1 + O(\mu^2, \beta^2), \quad (1.12)$$

$$\alpha^2 = \frac{1}{1 - \beta^2} \left[ 1 + \frac{2\varepsilon^2}{1 + \beta} \right] = 1 + O(\varepsilon^2, \beta^2), \quad (1.13)$$

$$\bar{\Omega} = \frac{2 + (2 + \eta)\mu^2}{2\sqrt{1 + \mu^2}} \sqrt{1 - \beta^2} = 1 + O(\mu^2, \beta^2), \quad (1.14)$$

and we have rescaled as follows

$$\begin{aligned} \chi t = t^*, \quad s = s^*, \quad \alpha \bar{z} = z^*, \\ u = u^*, \quad v = v^*, \quad \alpha w = w^*, \quad \frac{\alpha^2}{\chi} p = p^*. \end{aligned}$$

At this point, we specialise the analysis to consider both distortion measures  $\varepsilon$  and  $\beta$  as being small. In fact, this is not at all restrictive, requiring only that *one of the physical parameters*  $\Omega_1$  or  $\eta$  *is small*. This is best understood physically. If the container is nearly a sphere  $\eta \ll 1$ , the flow is always close to uniform rotation regardless of the tipover angle  $\tan^{-1} \mu$  of the vorticity and hence of the precession rate. Similarly for a low precession rate but finite oblateness  $\eta$ , the tipover angle for the vorticity is only small and again deviations from circular streamlines are slight.

Three parameter sub-ranges are of particular interest. For the Earth,

$$\Omega_1 = 4 \times 10^{-8} \ll \eta \approx \frac{1}{200} \ll 1,$$

which implies that

$$\mu = 1.6 \times 10^{-5} \ll 1, \text{ and } \varepsilon^2 \ll \beta \ll \varepsilon \ll 1. \quad (1.15)$$

As noted before, here the shearing strain dominates the elliptical strain. Experimentally, past studies have taken  $\eta \ll 1$  and  $\mu$  as  $O(1)$  (Malkus, 1968,  $\eta \approx 1/12$  and  $\mu \approx 0.3$ ) which is the situation  $\Omega_1 = O(\eta) \ll 1$ . In this case,

$$\beta = O(\varepsilon) \ll 1. \quad (1.16)$$

Lastly for the exact linear and quadratic disturbances we consider in Section 4,  $\Omega_1 \ll \eta = O(1)$ , which means

$$\mu = O(\Omega_1) \ll 1, \text{ and } \beta = O(\varepsilon^2) \ll \varepsilon = O(\Omega_1) \ll 1. \quad (1.17)$$

For clarity, we focus upon the first and last cases where  $\mu \ll 1$  which forces a clear separation in orders between the shearing instability growth rates and their elliptical counterparts. Both scenarios are encompassed by the hierarchy

$$\varepsilon^2, \beta \ll \varepsilon \ll 1, \quad (1.18)$$

but are distinguished by the relative magnitude of  $\varepsilon^2$  with  $\beta$ . The smallness of  $\mu$  allows us to drop the rescaling factors listed in (1.12)–(1.14), that is, we may take

$$\bar{\Omega} = \alpha^2 = \chi = 1,$$

without losing any of the leading order behaviour. This simplification cannot be made in the experimental parameter range making analysis here messier. However, the elliptical coupling calculation is much simplified in this case because  $\varepsilon^2 \ll \beta$  as will emerge later. For the remainder of this asymptotic analysis, we take  $\Omega_1 \ll \eta = O(1)$  or in other words  $\mu$  is small. This puts us in the desired asymptotic regime, regardless of the geometry  $\eta$ , allowing connection with the exact linear solution work of Section 4.

We now divide  $\mathcal{L}$  into its two natural parts by defining the shearing operator  $\mathcal{L}_S$  and elliptical operator  $\mathcal{L}_E$  as follows

$$\begin{aligned} \mathcal{L} = & e^{i(\phi+t)} \mathcal{L}_S(\mathbf{u}, p) + e^{-i(\phi+t)} \mathcal{L}_S^+(\mathbf{u}, p) \\ & + e^{2i(\phi+t)} \mathcal{L}_E(\mathbf{u}, p) + e^{-2i(\phi+t)} \mathcal{L}_E^+(\mathbf{u}, p), \end{aligned} \quad (1.19)$$

where  $^+$  indicates complex conjugate. These may be written individually as

$$\mathcal{L}_S(\mathbf{u}, p) = \varepsilon \{ [\mathcal{M} \bar{\nabla} p + \mathcal{R} \mathbf{u}] + O(\Omega/\eta, \mu^2, \beta) \} \quad (1.20)$$

with

$$\bar{\nabla} = \bar{s} \frac{\partial}{\partial s} + \bar{\phi} \frac{1}{s} \frac{\partial}{\partial \phi} + \bar{z} \frac{\partial}{\partial \bar{z}}, \quad \mathcal{M} = \begin{bmatrix} 0 & 0 & 1 \\ 0 & 0 & i \\ 1 & i & 0 \end{bmatrix}, \quad \mathcal{R} = \begin{bmatrix} 0 & 0 & -i \\ 0 & 0 & 1 \\ -i & -1 & 0 \end{bmatrix},$$

and

$$\mathcal{L}_E(\mathbf{u}, p) = - \left\{ \mathcal{N} \left[ \left( \frac{1}{2} \beta + \varepsilon^2 \right) \bar{\nabla} p + i \varepsilon^2 \mathbf{u} \right] + O(\varepsilon^2 \Omega_3/\eta, \varepsilon^2 \beta, \mu^2 \varepsilon^2) \right\} \quad (1.21)$$

with

$$\mathcal{N} = \begin{bmatrix} 1 & i & 0 \\ i & -1 & 0 \\ 0 & 0 & 0 \end{bmatrix}.$$

Note that the elliptical operator does not vanish when  $\beta$  is set to 0 because the shearing strain contributes at second order to it. If we retain only the leading order form of each operator, the system of equations for a small disturbance become

$$\begin{aligned} \frac{\partial \mathbf{u}}{\partial t} + 2 \begin{bmatrix} -v \\ u \\ 0 \end{bmatrix} + \bar{\nabla} p = \varepsilon \{ e^{i(\phi+t)} [\mathcal{M} \bar{\nabla} p + \mathcal{R} \mathbf{u}] + e^{-i(\phi+t)} [\mathcal{M}^+ \bar{\nabla} p + \mathcal{R}^+ \mathbf{u}] \} \\ - \frac{1}{2} \beta \left\{ e^{2i(\phi+t)} \mathcal{N} \left[ \left( 1 + \frac{2\varepsilon^2}{\beta} \right) \bar{\nabla} p + i \frac{2\varepsilon^2}{\beta} \mathbf{u} \right] \right. \\ \left. + e^{-2i(\phi+t)} \mathcal{N}^+ \left[ \left( 1 + \frac{2\varepsilon^2}{\beta} \right) \bar{\nabla} p - i \frac{2\varepsilon^2}{\beta} \mathbf{u} \right] \right\}, \end{aligned} \quad (1.22)$$

$$\nabla \cdot \mathbf{u} = 0, \quad (1.23)$$

$$\mathbf{u} \cdot \hat{\mathbf{n}}|_{\partial V} = 0, \quad \text{with } \partial V: s^2 + (1 + \eta)z^2 = 1. \quad (1.24)$$

The reader should note that the original geometry has been recovered in the limit  $\mu \ll 1$ . The above set of equations forms the basis for the following two sections. With no precession, (1.22)–(1.24) is the normal mode problem for a uniformly-rotating basic state within a spheroidal container. The solutions are neutral oscillations called Poincaré modes (e.g. Greenspan, 1968). The terms on the right-hand side of (1.22) represent the leading order consequences of switching precession on. They act as

coupling terms which allow the Poincaré modes to interact. This interaction can become resonant in two particular instances leading to exponential growth of the two modes. The first such instance, we call a shearing instability after its cause; the shearing of the streamlines in their plane. This aspect of the basic flow is responsible for the operators  $\mathcal{L}_S$  and  $\mathcal{L}_S^+$  which resonantly couple two Poincaré modes when their azimuthal wavenumbers and frequencies differ by 1. Two modes may also be unstable through an elliptical instability when their azimuthal wavenumbers and frequencies differ by 2. The situation here is a little more involved because as well as the operators  $\mathcal{L}_E$  and  $\mathcal{L}_E^+$  being responsible, the shearing operator also contributes at its second order. Leaving this latter effect aside for a moment, one should still note that  $\mathcal{L}_E$  differs from the operator which appears in the analyses of elliptically-distorted containers (Waleffe, 1989; Kerswell, 1993b) obtained by setting  $\varepsilon$  to 0. However this difference will only lead to quantitative changes in the growth rate. Moreover, in the important limit  $\eta \ll 1$  which forces

$$\varepsilon^2/\beta \ll 1,$$

both effects become of lower order.

With this in mind, we focus upon the novel shearing instability in the following section. Here we illustrate how two Poincaré modes may be resonantly coupled through the operators  $\mathcal{L}_S$  and  $\mathcal{L}_S^+$  to produce this instability, and then go on to demonstrate the existence of such resonances for specific geometries. The analysis is exactly similar for elliptical coupling, examples of which have already been reported (Kerswell, 1993b).

## 2. THE SHEARING INSTABILITY

A Poincaré mode  $[\mathbf{u}(\mathbf{x}, t), p(\mathbf{x}, t)] = [\mathbf{Q}(\mathbf{x}), \Phi(\mathbf{x})]e^{i\lambda t}$  satisfies the system (1.22)–(1.24) when  $\varepsilon = \beta = 0$ . In an oblate spheroidal container

$$r^2 + (1 + \eta)z^2 = r^2 + \frac{z^2}{c^2} = 1,$$

these modes take the form

$$\mathbf{Q} = \begin{bmatrix} \frac{-i}{4 - \lambda^2} \left( \lambda \Phi_r + \frac{2m}{r} \Phi \right) \\ \frac{1}{4 - \lambda^2} \left( 2\Phi_r + \frac{m\lambda}{r} \Phi \right) \\ \frac{i}{\lambda} \Phi_z \end{bmatrix} e^{i(m\phi + \lambda t)} \quad (2.1)$$

where  $p = \Phi(r, z)e^{i(m\phi + \lambda t)}$  and, ignoring normalisation constants,

$$\Phi_{n,m,k} = r^{|m|} z^v \prod_{j=1}^N \left\{ \bar{x}_j^2 (\bar{x}_j^2 - 1) + \bar{x}_j^2 \left( \frac{r}{A_{n,m,k}} \right)^2 + (1 - \bar{x}_j^2) \left( \frac{z}{B_{n,m,k}} \right)^2 \right\}. \quad (2.2)$$

Here

$$A_{n,m,k}^2 = \frac{c^2 + (1 - c^2)(1 - \lambda^2/4)}{1 - \lambda^2/4}, \quad B_{n,m,k}^2 = \frac{c^2 + (1 - c^2)(1 - \lambda^2/4)}{\lambda^2/4}, \quad (2.3)$$

$$v = \begin{cases} 0, & \text{if } n - |m| \text{ even,} \\ 1, & \text{if } n - |m| \text{ odd,} \end{cases}$$

and  $\bar{x}_j^2$  are the  $N = \frac{1}{2}(n - |m| - v)$  distinct squared zeros of the associated Legendre polynomial  $P_n^{|m|}(\bar{x})$  in the open interval  $(0, 1)$ . The no-normal-velocity boundary condition reduces to the following algebraic problem for the eigenfrequency  $\lambda$

$$v + 2 \sum_1^N \frac{\lambda^2 c^2}{\lambda^2 c^2 - \bar{x}_j^2 \{4 - \lambda^2(1 - c^2)\}} = \frac{mc^2 \lambda}{2 - \lambda} \quad (2.4)$$

when  $m \geq 0$  and is extendable to  $m < 0$  by the relationship  $\lambda_{n,-m,k} = -\lambda_{n,m,k}$ . The subscript  $k$  labels the particular eigenfrequency and has a maximum value

$$k_{\max}(n, m) = \begin{cases} n - 1, & \text{if } m = 0, \\ n - |m|, & \text{if } m \neq 0, \end{cases} \quad (2.5)$$

in particular,  $k_{\max}(n, \pm n) = 0$ ; there are no Poincaré modes with  $n = |m|$ . The pressure function given in (2.2) was actually derived as the product of two associated Legendre functions in a 'modified' oblate spheroidal coordinate system by Bryan (1889). His work built upon the more general study undertaken by Poincaré (1885) of the oscillations possessed by self-gravitating ellipsoids. The alternative and more useful polynomial representation (2.2) was noted by Cartan (1922) and later by Kudlick (1966), Aldridge and Toomre (1969), and Greenspan (1968, p 65).

For  $\varepsilon \neq 0$  (ignoring  $\beta$  effects for this section), we consider a disturbance to the flow (1.6) which consists of two Poincaré modes to leading order in  $\varepsilon$

$$\mathbf{u} = A(t)\mathbf{Q}_a + B(t)\mathbf{Q}_b + \varepsilon \mathbf{u}_1 + O(\varepsilon^2).$$

The time-varying amplitudes,  $A$  and  $B$ , are defined such that

$$A = \langle \mathbf{Q}_a, \mathbf{u} \rangle \quad \text{and} \quad B = \langle \mathbf{Q}_b, \mathbf{u} \rangle$$

where

$$\langle \mathbf{Q}, \mathbf{u} \rangle = \iiint dV \mathbf{Q}^* \cdot \mathbf{u}$$

and the Poincaré modes are assumed normalised; in particular  $\langle \mathbf{Q}_a, \mathbf{u}_1 \rangle = \langle \mathbf{Q}_b, \mathbf{u}_1 \rangle = 0$ . Equation (1.22) may be alternately projected onto  $\mathbf{Q}_a$  and  $\mathbf{Q}_b$  giving the expressions

$$\frac{\partial A}{\partial t} - i\lambda_a A = \varepsilon \langle \mathbf{Q}_a, e^{i(\phi+t)} [\mathcal{M}\bar{\nabla}p_b + \mathcal{R}\mathbf{Q}_b] + e^{-i(\phi+t)} [\mathcal{M}^*\bar{\nabla}p_b + \mathcal{R}^*\mathbf{Q}_b] \rangle B,$$

and

$$\frac{\partial B}{\partial t} - i\lambda_b B = \varepsilon \langle \mathbf{Q}_b, e^{i(\phi+t)} [\mathcal{M}\bar{\nabla}p_a + \mathcal{R}\mathbf{Q}_a] + e^{-i(\phi+t)} [\mathcal{M}^*\bar{\nabla}p_a + \mathcal{R}^*\mathbf{Q}_a] \rangle A. \quad (2.6)$$

If the azimuthal dependence is separated in the Poincaré modes as follows

$$\mathbf{Q}_a = [u_a, v_a, w_a]^T e^{im_a\phi}, \quad \mathbf{Q}_b = [u_b, v_b, w_b]^T e^{im_b\phi},$$

the matrix elements in the expressions (2.6) will vanish unless  $m_a$  and  $m_b$  differ by 1; to be specific we assume  $m_b = m_a + 1$ . These matrix elements may then be written as

$$\begin{aligned} \langle \mathbf{Q}_a, e^{-i\phi} [\mathcal{M}^*\bar{\nabla}p_b + \mathcal{R}^*\mathbf{Q}_b] \rangle &= (1 + \lambda_b)I, \\ \langle \mathbf{Q}_b, e^{i\phi} [\mathcal{M}\bar{\nabla}p_a + \mathcal{R}\mathbf{Q}_a] \rangle &= (1 + \lambda_a)I^*, \end{aligned} \quad (2.7)$$

where  $I$  is found to be

$$I = i \iiint dV \left\{ \frac{1}{\lambda_b(2 + \lambda_a)} \frac{\partial \Phi_b}{\partial z} \left( \frac{\partial \Phi_a}{\partial r} - \frac{m_a}{r} \Phi_a \right) - \frac{1}{(2 - \lambda_b)\lambda_a} \frac{\partial \Phi_a}{\partial z} \left( \frac{\partial \Phi_b}{\partial r} + \frac{m_b}{r} \Phi_b \right) \right\}. \quad (2.8)$$

Searching for a solution of the form

$$A = A_0 \exp[(\bar{\sigma} - \frac{1}{2}i)t], \quad B = B_0 \exp[(\bar{\sigma} - \frac{1}{2}i)t]$$

leads to the equations

$$\begin{aligned} \left[ \bar{\sigma} - \left( \frac{1}{2} + \lambda_a \right) i \right] A_0 &= \varepsilon(1 - \lambda_b)I B_0, \\ \left[ \bar{\sigma} + \left( \frac{1}{2} - \lambda_b \right) i \right] B_0 &= \varepsilon(1 + \lambda_a)I^* A_0, \end{aligned} \quad (2.9)$$

and the conclusion that

$$\bar{\sigma} = \frac{i(\lambda_a + \lambda_b)}{2} \pm \sqrt{\varepsilon^2(1 + \lambda_a)(1 - \lambda_b)|I|^2 - \frac{1}{4}(\lambda_b - \lambda_a - 1)^2}. \quad (2.10)$$

There is exponential growth on a timescale  $\varepsilon$  if

$$-2\varepsilon\sqrt{(1 + \lambda_a)(1 - \lambda_b)}|I| < \lambda_b - \lambda_a - 1 < 2\varepsilon\sqrt{(1 + \lambda_a)(1 - \lambda_b)}|I|.$$

In particular, the growth rate is

$$\bar{\sigma} = \sigma\varepsilon = \sqrt{(1 + \lambda_a)(1 - \lambda_b)}|I|\varepsilon$$

when the modes are perfectly turned at  $\lambda_b = \lambda_a + 1$ .

Aside from this frequency condition and the azimuthal wave number prerequisite  $m_b = m_a + 1$ , a further condition must be satisfied if resonance is to occur; the interaction integral  $I$  of (2.8) vanishes unless  $n_b = n_a$  [ $n$  is the modal degree; see the pressure function definition (2.2)]. The explanation for this additional criterion is detailed in Appendix A. Briefly, a Poincaré mode of index  $n$  cannot ‘reach’ other modes of different indices through the operators  $\mathcal{L}_S$  or  $\mathcal{L}_S^+$  (or similarly through  $\mathcal{L}_E$  or  $\mathcal{L}_E^+$ ). Appendix A discusses this result in terms of the partitioning of the Poincaré modes into non-interacting spaces of equal  $n$ -index. The reader should also note the restriction on the range of the frequencies  $\lambda_b$  and  $\lambda_a$ . We require  $\lambda_b > 0$  and  $\lambda_a < 0$  for instability.

Formally the shearing instability is one of parametric resonance where the periodic forcing is due to the distorted basic state, however the condition for resonant coupling between two Poincaré modes is essentially that of a triad interaction. The ‘third wave’ is the distortion of the basic state which has frequency 1 and azimuthal wavenumber 1 with respect to the rotating frame. For elliptical instability, the ‘third wave’ of the basic state possesses a frequency of 2 and azimuthal wavenumber 2 and the resonance conditions are modified accordingly.

## 2.1 Coupling

Demonstrating the existence of these shearing resonances amounts to scanning geometries  $\eta$  for a particular chosen pair of modes until the coupling criteria are met. In contrast to the elliptical case, there is no simple sub-harmonic resonance due to the azimuthal condition  $m_b = m_a + 1$ ; this cannot be satisfied by  $m_b = m, m_a = -m$  where  $m$  is an integer. As a result there is no special subset of resonances in which a Poincaré mode interacts with its complex conjugate as exploited in Kerswell (1993b). Rather, we illustrate the general situation by selecting two simple families of couplings and determining their critical geometries and growth rates. The first family of couplings, between  $\Phi_{m+2, m, 1}$  and  $\Phi_{m+2, m+1, 1}$ , is chosen because the resonant geometry may be

easily determined. The two modes are

$$\Phi_a = \Phi_{m+2,m,1} = r^m \left\{ \bar{x}^2 (\bar{x}^2 - 1) + \bar{x}^2 \left( \frac{r}{A} \right)^2 + (1 - \bar{x}^2) \left( \frac{z}{B} \right)^2 \right\}$$

where  $\bar{x}$  is the sole root of  $P_{m+2}^m(\bar{x}) = 0$  in  $(0, 1)$  with frequency

$$\lambda_a = \frac{2(1 - \sqrt{1 + m\bar{x}^2 [m\bar{x}^2 + mc^2(1 - \bar{x}^2) + 2]})}{m\bar{x}^2 + mc^2(1 - \bar{x}^2) + 2} < 0,$$

and  $\Phi_b = \Phi_{m+2,m+1,1} = zr^{m+1}$  with frequency

$$\lambda_b = \frac{2}{1 + (m+1)c^2}, \quad m > 0.$$

Resonances, in terms of the critical geometry

$$c = \frac{1}{\sqrt{1 + \eta}}$$

and frequency  $\lambda_b$  are tabulated in Table 1 accompanied by the corresponding growth rate scaled by the strain  $\varepsilon$ . Table 2 lists a selection of resonances from the other chosen family of couplings between  $\Phi_{n,0,k_a}$  and  $\Phi_{n,1,k_b}$ . Figure 1 displays all the resonances of Table 1 and the set of resonances between  $\Phi_{n,0,k_a}$  and  $\Phi_{n,1,k_b}$  for which  $n = 1, \dots, 16$ ,  $k_a$  and  $k_b$  are either 1 or 2, and  $c < 3$ .

**Table 1** Resonances between  $\Phi_{m+2,m,1}$  and  $\Phi_{m+2,m+1,1}$  modes for  $m = 1, \dots, 13$ .

$m$	$\lambda_b$	$c$	$\sigma$
1	0.8220	0.8465	0.3531
2	0.7604	0.7371	0.4238
3	0.7302	0.6593	0.4553
4	0.7124	0.6012	0.4728
5	0.7007	0.5559	0.4838
6	0.6925	0.5194	0.4914
7	0.6863	0.4891	0.4969
8	0.6816	0.4636	0.5011
9	0.6778	0.4417	0.5044
10	0.6748	0.4225	0.5071
11	0.6722	0.4057	0.5093
12	0.6701	0.3907	0.5111
13	0.6682	0.3773	0.5126



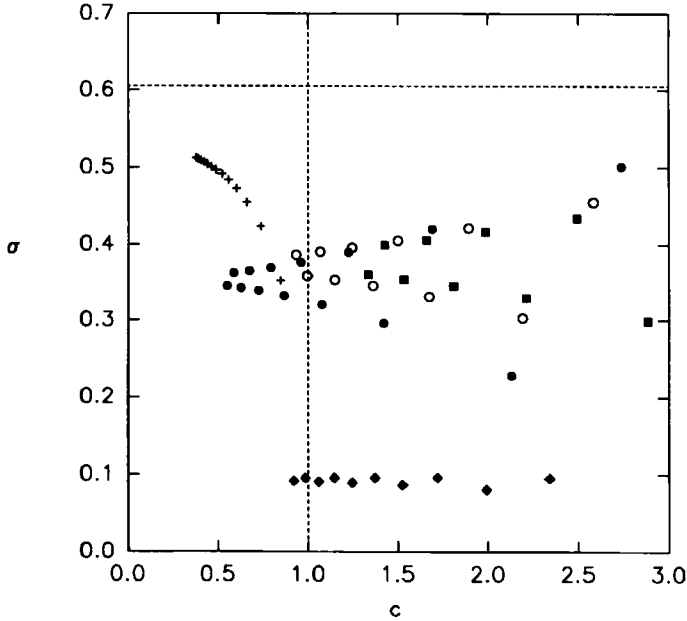


**Figure 1** A plot of the scaled growth rate  $\sigma = \bar{\sigma}/\varepsilon$  against the spheroidal geometry  $c = 1/\sqrt{1+\eta}$  for the resonances tabulated in Tables 1 and 2. Representing the resonance between the modes  $\Phi_{n,0,k_a}$  and  $\Phi_{n,1,k_b}$  by the label  $(n, k_a, k_b)$ , the solid circles represent  $(n, 1, 1)$  resonances; the solid squares  $(n, 2, 2)$  resonances;  $(n, 1, 2)$  for  $n$  even and  $(n, 2, 1)$  for  $n$  odd are plotted as hollow circles;  $(n, 2, 1)$  for  $n$  even and  $(n, 1, 2)$  for  $n$  odd are plotted as solid diamonds. Crosses are the  $\Phi_{m+2m1}$  &  $\Phi_{m+2m+1}$  resonances. The supremum value deduced in the unbounded analysis is shown by the horizontal dotted line. The spherical geometry is marked by the vertical dotted line.

### 3. THE ELLIPTICAL INSTABILITY

If  $\eta \ll 1$  ( $\varepsilon^2 \ll \beta$ ), an elliptical resonance can be treated in isolation from the shearing effects. To leading order, the elliptical coupling operator reduces to the familiar form *and* second order shearing effects are negligible. Elliptical growth rates are then identical to previous elliptical instability computations (Kerswell 1992, 1993b).

Capturing the leading order elliptical resonance is a little more involved when  $\eta = O(1)$  [i.e.  $\varepsilon^2 = O(\beta)$ ] because then the shearing operator contributes at its second order to the leading order calculation. In this case we start with a velocity expansion

$$\mathbf{u} = A\mathbf{Q}_a + B\mathbf{Q}_b + \varepsilon\{\mathbf{v}_{11}e^{i(\lambda_a-1)t} + \mathbf{v}_{12}e^{i(\lambda_a+1)t} + \mathbf{v}_{13}e^{i(\lambda_b+1)t}\} + \beta\mathbf{v}_2 + O(\varepsilon\beta), \quad (3.1)$$

where

$$\mathbf{v}_{11}(\mathbf{x}) = \hat{\mathbf{v}}_{11}(r, z)e^{i(m_a-1)\phi}, \quad \mathbf{v}_{12}(\mathbf{x}) = \hat{\mathbf{v}}_{12}(r, z)e^{i(m_a+1)\phi}, \quad \mathbf{v}_{13}(\mathbf{x}) = \hat{\mathbf{v}}_{13}(r, z)e^{i(m_b+1)\phi}.$$

**Table 2** A selection of resonances between  $\Phi_{n,0,k_a}$  and  $\Phi_{n,1,k_b}$ .

$n$	$k_a$	$k_b$	$\lambda_b$	$c$	$\sigma$
3	1	1	0.6406	2.7371	0.5009
4	1	1	0.2468	2.1302	0.2281
5	1	1	0.6536	1.6925	0.4204
6	1	1	0.3000	1.4207	0.2961
7	1	1	0.6560	1.2260	0.3903
8	1	1	0.3186	1.0754	0.3212
9	1	1	0.6567	0.9618	0.3769
10	1	1	0.3272	0.8667	0.3330
10	2	1	0.1800	1.5242	0.0865
10	1	2	0.5960	1.5012	0.4053
10	2	2	0.4082	2.2120	0.3299
11	1	1	0.6569	0.7917	0.3698
11	2	1	0.3902	1.3614	0.3459
11	1	2	0.7999	1.3707	0.0960
11	2	2	0.5714	1.9865	0.4167
12	1	1	0.3319	0.7263	0.3395
12	2	1	0.1901	1.2452	0.0894
12	1	2	0.5955	1.2465	0.3961
12	2	2	0.4164	1.8077	0.3458
13	1	1	0.6570	0.6729	0.3657
13	2	1	0.3948	1.1491	0.3540
13	1	2	0.7963	1.1442	0.0957
13	2	2	0.5703	1.6583	0.4063
14	1	1	0.3348	0.6252	0.3435
14	2	1	0.1961	1.0563	0.0909
14	1	2	0.5952	1.0669	0.3904
14	2	2	0.4211	1.5332	0.3550
15	1	1	0.6571	0.5853	0.3630
15	2	1	0.3976	0.9951	0.3590
15	1	2	0.7941	0.9840	0.0956
15	2	2	0.5695	1.4261	0.3997
16	1	1	0.3366	0.5489	0.3461
16	2	1	0.2000	0.9188	0.0919
16	1	2	0.5949	0.9332	0.3867
16	2	2	0.4240	1.3332	0.3609

Defining

$$\mathcal{L}_0(\mathbf{u}, p) = \frac{\partial \mathbf{u}}{\partial t} + 2[-v, u, 0]^T + \bar{\mathbf{V}}p,$$

we have the 3 inhomogeneous problems,

$$\begin{aligned} \mathcal{L}_0(\mathbf{v}_{11}, p_{11}) &= Ae^{-i(\phi+t)} \mathcal{L}_S^+(\mathbf{Q}_a, p_a), \\ \mathcal{L}_0(\mathbf{v}_{12}, p_{12}) &= Ae^{i(\phi+t)} \mathcal{L}_S(\mathbf{Q}_a, p_a) + Be^{-i(\phi+t)} \mathcal{L}_S^+(\mathbf{Q}_b, p_b), \\ \mathcal{L}_0(\mathbf{v}_{13}, p_{13}) &= Be^{i(\phi+t)} \mathcal{L}_S(\mathbf{Q}_b, p_b), \end{aligned} \tag{3.2}$$

at  $O(\beta)$  to apparently solve. The two amplitude equations for  $A$  and  $B$  read

$$\begin{aligned} \frac{\partial A}{\partial t} - i\lambda_a A = \beta \langle \mathbf{Q}_a, e^{-2i(\phi+t)} \mathcal{L}_E^+(\mathbf{Q}_b, p_b) \rangle B \\ + \varepsilon^2 \{ \langle \mathbf{Q}_a, e^{-i(\phi+t)} \mathcal{L}_S^+(\mathbf{v}_{12}, p_{12}) \rangle + \langle \mathbf{Q}_a, e^{i(\phi+t)} \mathcal{L}_S(\mathbf{v}_{11}, p_{11}) \rangle \}, \end{aligned} \quad (3.3)$$

$$\begin{aligned} \frac{\partial B}{\partial t} - i\lambda_b B = \beta \langle \mathbf{Q}_b, e^{2i(\phi+t)} \mathcal{L}_E(\mathbf{Q}_a, p_a) \rangle A \\ + \varepsilon^2 \{ \langle \mathbf{Q}_b, e^{i(\phi+t)} \mathcal{L}_S(\mathbf{v}_{12}, p_{12}) \rangle + \langle \mathbf{Q}_b, e^{-i(\phi+t)} \mathcal{L}_S^+(\mathbf{v}_{13}, p_{13}) \rangle \}, \end{aligned} \quad (3.4)$$

to  $O(\beta)$ . Of the  $O(\varepsilon^2)$  matrix elements, only those containing  $\mathbf{v}_{12}$  are important: just the first order velocity  $\mathbf{v}_{12}$  allows the modes  $\mathbf{Q}_a$  and  $\mathbf{Q}_b$  to interact at the second order through the shearing operator. In contrast,  $\mathbf{v}_{11}$  and  $\mathbf{v}_{13}$  lead purely to  $O(\varepsilon^2)$  frequency shifts and can be ignored. Thus only the first order problem (3.2) need be solved. Appendix C contains an example of such a calculation.

#### 4. EXACT LINEAR SOLUTIONS

In this section we construct some exact solutions to the linearised Euler equation describing the evolution of a disturbance upon Poincaré's basic solution in a precessing spheroid. The emphasis here is to provide an alternative demonstration of instability under finite rates of precession. In doing so, we are also able to corroborate the perturbation analysis presented above for small precession rates in some special cases. With this in mind, we keep the analysis as direct as possible by working in the precessing frame (where the  $z$ -axis is chosen to coincide with the spheroidal axis of symmetry) and by considering simple, *exact*, linear solutions which are valid for *arbitrary* precession rates.

The component of the precessional vector parallel to the container's angular velocity is unimportant so we take  $\boldsymbol{\Omega} = \Omega \hat{\mathbf{x}}$  (that is  $\Omega_1 = \Omega$  and  $\Omega_3 = 0$ ). Poincaré's basic state can be written as

$$\mathbf{U} = \begin{bmatrix} 0 & -1 & 0 \\ 1 & 0 & -(1+\eta)\mu \\ 0 & \mu & 0 \end{bmatrix} \mathbf{x} = \mathbf{A} \cdot \mathbf{x} \quad (4.1)$$

where then  $\mu = 2\Omega/\eta$ . The linearised disturbance equations in the precessing frame are

$$\frac{\partial \mathbf{u}}{\partial t} + 2\Omega \times \mathbf{u} + \mathbf{A} \cdot \mathbf{x} \cdot \nabla \mathbf{u} + \mathbf{A} \cdot \mathbf{u} + \nabla p = \mathbf{0}, \tag{4.2}$$

$$\nabla \cdot \mathbf{u} = 0, \quad \mathbf{u} \cdot \hat{\mathbf{n}}|_{\partial V} = 0, \tag{4.3}$$

with

$$\partial V: x^2 + y^2 + \frac{z^2}{c^2} = 1 = x^2 + y^2 + (1 + \eta)z^2.$$

We now consider the eigensolutions,  $\mathbf{u}(\mathbf{x}, t) = \mathbb{Q}(\mathbf{x})e^{i\Lambda t}$ , where  $\Lambda$  is the eigenfrequency in the precessing frame, of this system as a function of  $\Omega$ . If the precession is turned off ( $\Omega = 0$ ), the eigensolutions are the Poincaré modal velocities  $\mathbf{Q}_{nmk}(\mathbf{x})e^{i\Lambda t}$ . The spatial components of these velocities naturally partition into orthogonal vector spaces  $\mathcal{V}_n$  where

$$\mathcal{V}_n = \langle \mathbf{Q}_{nmk}; -n \leq m \leq n, k = 1, \dots, k_{\max}(n, m) \rangle,$$

and  $\dim(\mathcal{V}_n) = n^2 - 1$  using (2.5), under the inner product

$$\langle \mathbf{Q}_a, \mathbf{Q}_b \rangle = \iiint \mathbf{Q}_a^+ \cdot \mathbf{Q}_b dV.$$

If we understand  $\mathbb{Q}_{nmk}$  to represent the image of the Poincaré eigensolution  $\mathbf{Q}_{nmk}$  as  $\Omega$  increases from zero, one would naively expect the disturbed eigensolutions  $\mathbb{Q}_{nmk}$  to be non-trivial superpositions of the  $\mathbf{Q}$ 's taken from various vector spaces  $\mathcal{V}_n$ . However, the actual situation is simpler than this: each eigensolution belongs to one and only one vector space which is invariant as  $\Omega$  changes. In other words,

$$\begin{aligned} \mathcal{V}_n &= \langle \mathbb{Q}_{nmk}; -n \leq m \leq n, k = 1, \dots, k_{\max}(n, m) \rangle \\ &= \langle \mathbf{Q}_{nmk}; -n \leq m \leq n, k = 1, \dots, k_{\max}(n, m) \rangle. \end{aligned}$$

Reworded, this statement means that a disturbance in  $\mathcal{V}_n$  at some time  $t$  will remain so for all subsequent times regardless of the value of  $\Omega$ . Appendix A proves this assertion.

Armed with this result, we can now construct exact solutions to the system (4.2) and (4.3) by considering general disturbances within each vector space  $\mathcal{V}_n$ . By the definition of these spaces, the Poincaré modal velocities are basis vectors and hence we may write the eigensolutions as

$$\mathbf{u}(\mathbf{x}, t) = \sum_{m,k} \alpha_{mk} \mathbf{Q}_{nmk}(\mathbf{x})e^{\sigma t}$$

where a  $\dim(\mathcal{V}_n) \times \dim(\mathcal{V}_n)$  matrix eigenvalue problem must be solved for  $\sigma$ . However, certainly for  $\mathcal{V}_2$  and  $\mathcal{V}_3$  upon which we are now to concentrate, it is easier to work with different bases.

#### 4.1 $\mathcal{V}_2$ : Linear velocities

The vector space  $\mathcal{V}_2$  represents the space of all incompressible velocities which are purely linear in the spatial coordinates and which satisfy the boundary conditions (see Appendix A). This is the space of spatially-constant vorticity solutions. There are 3 Poincaré modes which span this space,  $\mathbf{Q}_{2,-1,1}$ ,  $\mathbf{Q}_{2,0,1}$  and  $\mathbf{Q}_{2,1,1}$ . A suitable basis is

$$\mathbf{u}_1 = \frac{z}{c} \hat{y} - cy\hat{z}, \quad \mathbf{u}_2 = -\frac{z}{c} \hat{x} + cx\hat{z}, \quad \mathbf{u}_3 = y\hat{x} - x\hat{y}, \quad (4.4)$$

with each a vortical flow about one of the container axes. Every basis velocity  $\mathbf{u}_i$  is incompressible and individually obeys the boundary conditions so a disturbance of the form

$$\mathbf{u}(\mathbf{x}, t) = \sum_{i=1}^3 \alpha_i(t) \mathbf{u}_i(\mathbf{x}),$$

where the  $\alpha_i$ 's are spatially-constant, is required only to satisfy the vorticity equation [ $\nabla \times (4.2)$ ]. In this special case of constant-vorticity disturbances, the nonlinear terms may also be retained leading to the exact, viscous evolution system

$$\frac{\partial \alpha_1}{\partial t} = \kappa \alpha_2 (1 - \alpha_3), \quad \frac{\partial \alpha_2}{\partial t} = -\kappa \alpha_1 (1 - \alpha_3), \quad \frac{\partial \alpha_3}{\partial t} = -\chi \alpha_2. \quad (4.5)$$

where  $\kappa = (1 - c^2)/(1 + c^2)$  and  $\chi = \Omega c$ . This dynamical system may be reduced to second order by the transformation

$$\alpha_1 + i\alpha_2 = \zeta e^{i\Theta}, \quad \alpha_3 = \xi,$$

which leads to the equations

$$\frac{\partial \zeta}{\partial t} = 0, \quad \frac{\partial \Theta}{\partial t} = \kappa(\xi - 1), \quad \frac{\partial \xi}{\partial t} = -\chi \zeta \sin \Theta.$$

This system possesses oscillatory behaviour about  $\zeta = \xi = 0$  indicating overall stability of the flow. Hocking (1965) dealt with an associated problem of impulsively-started and—stopped precession by assuming that the response would be in terms of a spatially-constant, but time-dependent vortical flow, obtaining a similar system to (4.5). Greenspan (1968, p 176) treated large-angle precession in the same fashion, integrating his equations numerically to find oscillatory solutions.

Linearising the system (4.5) and inserting the ansatz

$$\alpha_i(t) = \alpha_i e^{\sigma t}$$

leads to the three eigenfrequencies

$$\sigma_1 = 0, \quad \sigma_2 = i\kappa, \quad \sigma_3 = -i\kappa$$

indicating linear stability. This, however, would seem to contradict the perturbation analysis which predicts a shearing instability between  $\mathbf{Q}_{2,0,1}$  and  $\mathbf{Q}_{2,1,1}$  and an elliptical instability between  $\mathbf{Q}_{2,-1,1}$  and  $\mathbf{Q}_{2,1,1}$  at some values of the geometry  $c$ . Consideration of the modal frequencies at the predicted resonances is sufficient to resolve this momentary paradox. Recall that the frequency of interest is that in the precessing, rotating frame of the container: we label this  $\lambda_{nmk}$ . The frequency  $\Lambda_{nmk}$  has been defined as the modal frequency in the precessing frame and therefore  $\lambda_{nmk} = \Lambda_{nmk} + m$  where  $m$  is the azimuthal wavenumber. Now  $\lambda_{2,0,1}$  is precisely 0 for all  $c$ : it is simply an extra rotation about  $\hat{\mathbf{z}}$ . So, at the shearing resonance,  $\lambda_{2,1,1}$  must be 1 which ensures that one of the interaction integrals between  $\mathbf{Q}_{2,0,1}$  and  $\mathbf{Q}_{2,1,1}$  vanishes [see (2.7)]. For  $\mathbf{Q}_{2,-1,1}$  and  $\mathbf{Q}_{2,1,1}$  to couple elliptically,  $\lambda_{2,1,1}$  must equal 1, implying  $\eta = 0$  and the spheroid is a sphere. This is the one geometry in which an inviscid fluid cannot feel precession of its boundary and so there are no strains to excite these waves elliptically. We must consider quadratic disturbances to capture instability.

#### 4.2 $\mathcal{V}_3$ : Quadratic velocities

The vector space  $\mathcal{V}_3$  represents the space of all incompressible, quadratic velocities which satisfy the boundary conditions. Its Poincaré modal basis is

$$\{\mathbf{Q}_{3,-2,1}, \mathbf{Q}_{3,-1,1}, \mathbf{Q}_{3,-1,2}, \mathbf{Q}_{3,0,1}, \mathbf{Q}_{3,0,2}, \mathbf{Q}_{3,1,1}, \mathbf{Q}_{3,1,2}, \mathbf{Q}_{3,2,1}\} \quad (4.6)$$

where, if  $\Omega = 0$ ,

$$\lambda_{3,2,1} = -\lambda_{3,-2,1} = \frac{2}{2c^2 + 1} > 0,$$

$$\lambda_{3,1,1} = -\lambda_{3,-1,1} = \frac{10 + 4\sqrt{9 + c^2}}{4c^2 + 11} > 0,$$

$$\lambda_{3,1,2} = -\lambda_{3,-1,2} = \frac{10 - 4\sqrt{9 + c^2}}{4c^2 + 11} < 0,$$

$$\lambda_{3,0,1} = -\lambda_{3,0,2} = -\frac{2}{\sqrt{4c^2 + 1}} < 0.$$

We use the same basis for this space as Gledzer and Ponomarev (1992) who studied the quadratic velocity instability within an elliptically-distorted spheroid. This basis is

$$\mathbf{v}_1 = (y^2 - z^2/c^2)\hat{\mathbf{x}} - xy\hat{\mathbf{y}} + xz\hat{\mathbf{z}},$$

$$\mathbf{v}_2 = (1 - x^2 - 2y^2 - 2z^2/c^2)\hat{\mathbf{x}} + xy\hat{\mathbf{y}} + xz\hat{\mathbf{z}},$$

$$\mathbf{v}_3 = xy\hat{\mathbf{x}} + (z^2/c^2 - x^2)\hat{\mathbf{y}} - yz\hat{\mathbf{z}},$$

$$\mathbf{v}_4 = xy\hat{\mathbf{x}} + (1 - 2x^2 - y^2 - 2z^2/c^2)\hat{\mathbf{y}} + yz\hat{\mathbf{z}},$$

$$\mathbf{v}_5 = -(xz/c^2)\hat{\mathbf{x}} + (yz/c^2)\hat{\mathbf{y}} + (x^2 - y^2)\hat{\mathbf{z}},$$

$$\mathbf{v}_6 = (xz/c^2)\hat{\mathbf{x}} + (yz/c^2)\hat{\mathbf{y}} + (1 - 2x^2 - 2y^2 - z^2/c^2)\hat{\mathbf{z}},$$

$$\mathbf{v}_7 = (yz/c^2)\hat{\mathbf{x}} - xy\hat{\mathbf{z}},$$

$$\mathbf{v}_8 = -(xz/c^2)\hat{\mathbf{y}} + xy\hat{\mathbf{z}}.$$

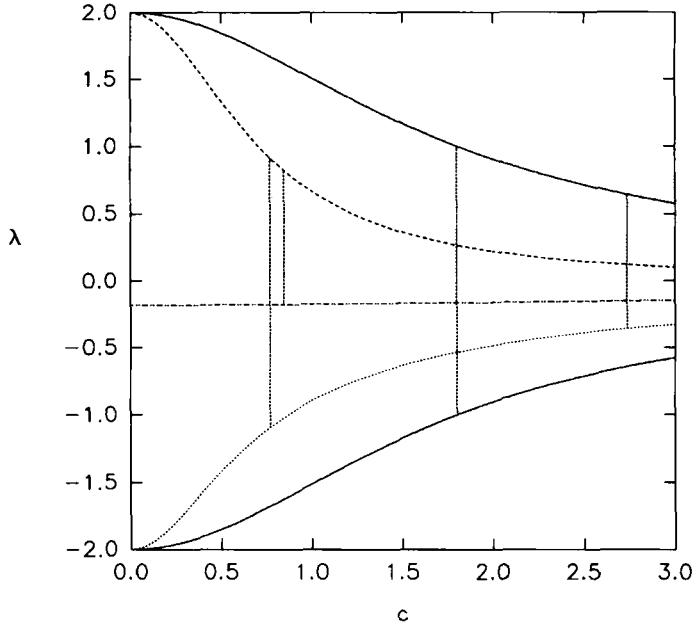


**Figure 2** The quadratic frequencies  $\lambda_{3,m,k}$  as a function of the geometry  $c$ . The uppermost (lowermost) solid curve represents  $\lambda_{3,1,1}$  ( $\lambda_{3,-1,1}$ ); the second highest, dashed curve  $\lambda_{3,2,1}$ ; the almost horizontal, dash-dot curve  $\lambda_{3,1,2}$  and underneath this, the dotted line  $\lambda_{3,0,1}$ . The vertical lines are either of length 1 or 2 in frequency and indicate where resonances occur between the modes. The four lines correspond to the four tongues which emanate from the  $\Omega$  axis in Figure 3.

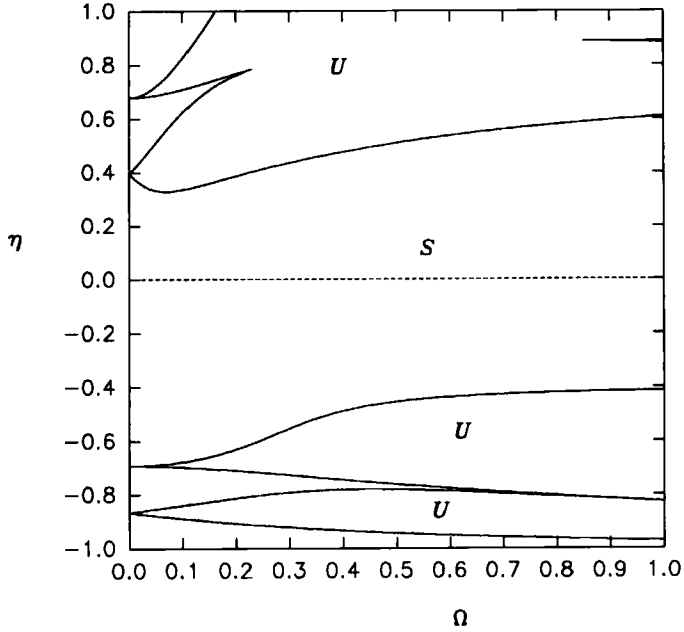


**Figure 3** The four instability tongues obtained for quadratic velocity disturbances (*U* indicates instability and *S* stability). The dotted line marks the spherical geometry.

Again these basis vectors are incompressible velocities which individually satisfy the boundary conditions. Substituting the eigensolution

$$\mathbf{u} = \sum_{i=1}^8 \alpha_i \mathbf{v}_i(\mathbf{x}) e^{\sigma t}$$

into the vorticity equation gives 8 equations (see Appendix B) and hence an  $8 \times 8$  matrix eigenvalue problem for  $\sigma$ . This eigenvalue problem depends on two parameters: the geometry  $\eta$  and the precession rate  $\Omega$ . Figure 3 maps out the regions of stability and instability relative to these two external parameters. There are 4 tongues of instability emanating from the  $\Omega = 0$  axis and each can be identified within the framework of the perturbation analysis.

Consider the set (4.6) and their eigenfrequencies plotted in Figure 2. We can expect a shearing instability to occur between  $\mathbf{Q}_{3,0,1}$  and  $\mathbf{Q}_{3,1,1}$  (along with the conjugate resonance between  $\mathbf{Q}_{3,0,2}$  and  $\mathbf{Q}_{3,-1,1}$ ) at  $\eta = -0.866523$  (the first entry in Table 2). This corresponds to the lowest tongue in Figure 3. The numerically-calculated growth rate within this tongue converges to the expected asymptotic value of  $\sigma = 0.500868 \varepsilon$  as  $\Omega \rightarrow 0$  to confirm this identification. A shearing instability can also occur between  $\mathbf{Q}_{3,1,2}$  and  $\mathbf{Q}_{3,2,1}$  at  $\eta = 0.3955096$  (the first entry in Table 1) with growth rate  $\sigma = 0.353092 \varepsilon$ : this identifies the third tongue.



The other two tongues are much thinner and hence indicate higher order instabilities. These are the elliptical couplings between  $\mathbf{Q}_{3,-1,1}$  and  $\mathbf{Q}_{3,1,1}$ , and between  $\mathbf{Q}_{3,0,1}$  and  $\mathbf{Q}_{3,2,1}$ . Both are straightforward to identify by their critical  $\eta$  values,  $\eta = -0.692308$  and  $\eta = 0.678574$ , and their asymptotic growth rates  $\sigma = 0.517852\beta$  and  $\sigma = 0.630487\beta$  respectively. The former growth rate is familiar from past work on elliptical instabilities (Gledzer and Ponomarev 1992; Kerswell, 1992), whereas the growth rate for the  $\mathbf{Q}_{3,0,1} - \mathbf{Q}_{3,2,1}$  coupling seems to contradict the assumed supremum of  $0.5625\beta$  (Kerswell, 1992). The reason is that in this case the shearing operator contributes at second order to the elliptical coupling as discussed in Section 3. We describe this particular calculation in Appendix C. The absence of shearing effects in the case of the coupling  $\mathbf{Q}_{3,-1,1} - \mathbf{Q}_{3,1,1}$  is due to the coincidence  $\lambda_{3,1,1} = 1$ : in this instance the effect of the shearing operator vanishes.

Other features of Figure 3 are worthy of note. Instability can only occur for  $c$  values which lie outside the range  $0.87 < c < 1.29$ . So both prolate and oblate spheroids are unstable provided their distortion from sphericity is sufficiently large. The coalescence of the instability tongues emerging from  $\eta = 0.3955096$  and  $\eta = 0.678574$  could suggest an interesting experimental study. A line drawn horizontally across the figure from  $(\Omega, \eta) = (0, \eta_s)$  where  $0.679 < \eta_s < 0.784$  ( $0.749 < c_s < 0.771$ ) starts off in a stable region then crosses the elliptical instability tongue  $\mathbf{Q}_{3,0,1} - \mathbf{Q}_{3,2,1}$ , becomes stable again and then enters the shearing instability tongue associated with  $\mathbf{Q}_{3,1,2} - \mathbf{Q}_{3,2,1}$  (The relevance of moving horizontally along the figure in the laboratory is its comparative ease relative to vertical motion). Of course, this simple picture ignores the presence of other tongues corresponding to different forms of disturbance. We should emphasize that such a figure indicates sufficient *not* necessary conditions for instability.

## 5. UNBOUNDED SHEARED, CIRCULAR STREAMLINES

In this section we consider a rotating, unbounded fluid whose rotation axis is precessing. The undisturbed, steady (in the precessing frame) state consists of sheared circular streamlines. In the absence of a confining boundary, no elliptical distortion is induced permitting a study of just the shearing strain generic to precessing flows. We demonstrate the local instability of these sheared circular streamlines to the straining field present, confirming that the effect of boundaries is largely secondary.

The unbounded flow to be considered is

$$\mathbf{u} = \begin{bmatrix} 0 & -1 & 0 \\ 1 & 0 & -2\varepsilon \\ 0 & 0 & 0 \end{bmatrix} \mathbf{x} = \mathbf{D} \cdot \mathbf{x} \quad (5.1)$$

which is an exact, incompressible, viscous solution of the Navier Stokes equation in a frame rotating at  $\Omega = \varepsilon \hat{\mathbf{x}}$ . The flow is rotating about the  $z$ -axis which is itself rotating slowly at  $\varepsilon$  about the  $x$ -axis. This gives rise to the same sheared circular streamlines

about the  $z$ -axis as produced within a precessing spheroid; see the flow (1.1) when  $\mu$  is only retained to first order.

An unbounded, uniformly rotating flow supports a spectrum of inertial oscillations consisting of travelling waves whose wave vectors rotate with the flow (e.g. Greenspan, 1968). Viewed from the inertial frame, these ‘Kelvin’ modes may be written as

$$[\mathbf{u}(\mathbf{x}, t), p(\mathbf{x}, t)] = [\hat{\mathbf{u}}(t), \hat{p}(t)] \exp(ik(t) \cdot \mathbf{x});$$

a form of sufficient generality to describe oscillations upon any flow with spatially uniform strain rates (Craik and Criminale, 1986, more recently Craik and Allen, 1992, and Bayly 1986 in his study of elliptical flow). For our strained, rotating flow, such a Kelvin mode is an exact, nonlinear, inviscid, incompressible solution upon the basic state if both

$$\frac{d\mathbf{k}}{dt} + \mathbf{D}^T \cdot \mathbf{k} = \mathbf{0}, \tag{5.2}$$

and

$$\frac{d\hat{\mathbf{u}}}{dt} + \mathbf{D} \cdot \hat{\mathbf{u}} + 2\boldsymbol{\Omega} \times \hat{\mathbf{u}} + ik\hat{p} = \mathbf{0}, \tag{5.3}$$

hold. The fluid is taken as inviscid for consistency with the bounded analysis although incorporating viscosity here is readily done. The first equation (5.2) has the solution

$$\mathbf{k} = k_0 \begin{bmatrix} \tan \alpha \cos t \\ \tan \alpha \sin t \\ 1 - 2\varepsilon \tan \alpha \cos t \end{bmatrix} \tag{5.4}$$

where  $\alpha$  is the average angle  $\mathbf{k}$  makes with the rotation axis. With this, equation (5.3) is a Floquet problem for  $\hat{\mathbf{u}}$ ,

$$\frac{d\hat{u}_i}{dt} = (2\boldsymbol{\Omega} \times \hat{\mathbf{u}})_j \left[ \frac{k_i k_j}{k^2} - \delta_{ij} \right] + \left[ \frac{2k_i k_j}{k^2} - \delta_{ij} \right] D_{ji} \hat{u}_i,$$

with only one free parameter; the angle  $\alpha$ . In particular, there is no dependence on  $|\mathbf{k}|$  and the problem is scale invariant as it must be with no inherent length scale in the problem. The search for instability proceeds in the standard way (e.g. see Joseph, 1976) by examining the eigenvalues  $\mu$  of the matrix  $\mathbf{M}(2\pi)$  defined by the problem

$$\frac{dM_{im}}{dt} = A_{ii} M_{im}, \quad \mathbf{M}(0) = \mathbf{I}, \tag{5.5}$$

with

$$A_{ii} = 2\varepsilon \left[ \frac{k_i k_j}{k^2} - \delta_{ij} \right] \epsilon_{1ij} + \left[ \frac{2k_i k_j}{k^2} - \delta_{ij} \right] D_{ji}.$$

Instability occurs if an eigenvalue has a modulus exceeding 1. A couple of observations are worthy of note. Firstly, the determinant of  $\mathbf{M}(2\pi)$  must be 1 because the time-averaged trace of the matrix  $\mathbf{A}$  is zero; and secondly

$$\frac{d}{dt}(k_i M_{ij}) = 0,$$

or in other words, as  $\mathbf{M}(0) = \mathbf{I}$ ,  $\mathbf{k}(0) = \mathbf{k}(2\pi)$  is a left-eigenvector of  $\mathbf{M}(2\pi)$  with an eigenvalue of 1. The remaining 2 eigenvalues are then either complex conjugates on the unit circle, indicating stability, or a real, reciprocal pair, one of which must lie outside the unit circle. This signals instability with a growth rate  $\bar{\sigma}$  calculated via

$$\bar{\sigma}(\alpha, \varepsilon) = \frac{1}{2\pi} \ln |\mu(\alpha, \varepsilon)|.$$

Figures 4 and 5 summarise the findings. For all  $\varepsilon \neq 0$ , there exists a band of angles in which the velocity amplitude  $\hat{u}$  grows exponentially. Figure 4 shows the (wide) subharmonic and (much narrower) higher order tongues of instability emerging from the axis  $\varepsilon = 0$  characteristic of parametric resonance. The main subharmonic tongue emanates from  $\alpha = \cos^{-1} 1/4 \approx 1.3181$  where the wavevector  $\mathbf{k}$  rotates once every two basic

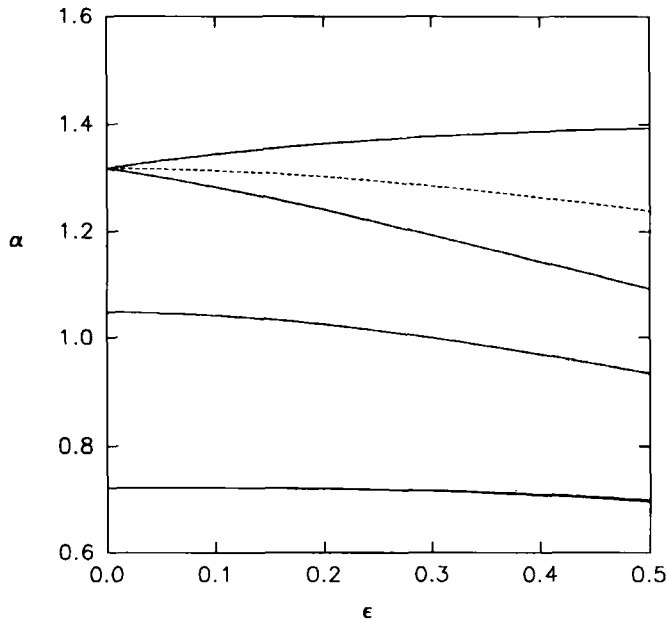


**Figure 4** The Floquet tongues of instability as a function of the strain  $\varepsilon$ . Within the subharmonic tongue emanating from  $\alpha = \cos^{-1} 1/4$ , the dashed line indicates the inclination  $\alpha$  of largest growth rate (plotted in Figure 5) at a given  $\varepsilon$ . The higher order tongues, starting from  $\alpha = \cos^{-1} 1/2$  and  $\cos^{-1} 3/4$  are so thin as to appear as lines here.

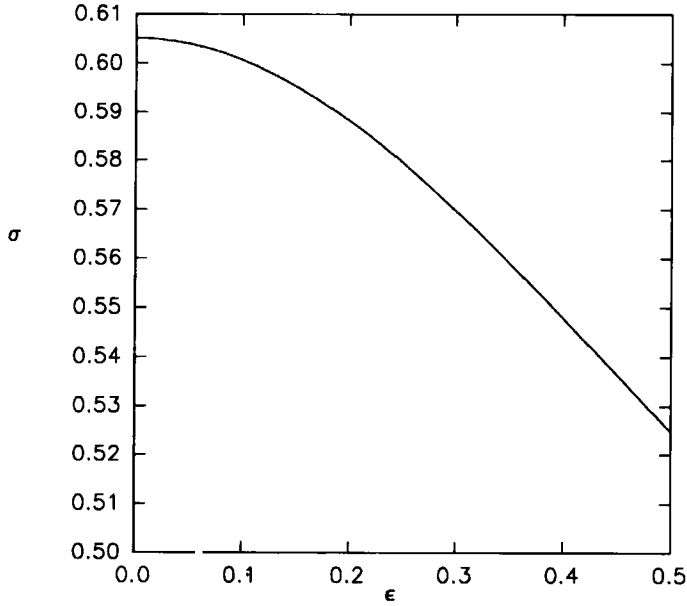


**Figure 5** A plot of the maximum scaled growth rate  $\sigma = \bar{\sigma}/\varepsilon$  against the strain  $\varepsilon$ . The intercept is  $\sigma = 5\sqrt{15/32}$ .

rotation periods. Subsequent tongues emerge from similar synchronisation points [e.g. the  $O(\varepsilon^2)$  tongue starts at  $\alpha = \cos^{-1} 1/2$  where the wavevector rotates on average with the basic flow]. Figure 5 describes how the maximum growth rate varies with  $\varepsilon$  within the subharmonic tongue. The limit  $\varepsilon \rightarrow 0$  corresponds to the scaled growth rate  $\sigma = \bar{\sigma}/\varepsilon = 5\sqrt{15/32} \approx 0.6052$ . The  $O(\varepsilon)$  asymptotic results for  $\varepsilon \ll 1$  may be verified analytically using the power statement

$$\frac{d}{dt} \left( \frac{1}{2} |\hat{\mathbf{u}}|^2 \right) = 2\varepsilon \hat{v} \hat{w} \quad (5.6)$$

obtained through the dot product of  $\hat{\mathbf{u}}$  with equation (5.3). For  $\varepsilon = 0$ , the Kelvin mode with wave vector inclined at  $\alpha$  to  $\hat{\mathbf{z}}$  and perpendicular to the straining at  $t = 0$ ,

$$\mathbf{k} = k_0 [-\tan \alpha \sin t, \tan \alpha \cos t, 1]^T,$$

is

$$\mathbf{u}_0 = \begin{bmatrix} \frac{\gamma-1}{2} \cos\left(\frac{2}{\gamma} + 1\right)t + \frac{\gamma+1}{2} \cos\left(1 - \frac{2}{\gamma}\right)t \\ \frac{\gamma-1}{2} \sin\left(\frac{2}{\gamma} + 1\right)t + \frac{\gamma+1}{2} \sin\left(1 - \frac{2}{\gamma}\right)t \\ \tan \alpha \sin\left(\frac{2}{\gamma}\right)t \end{bmatrix} \quad (5.7)$$

where  $1/\gamma = \cos \alpha$ . When  $0 < \varepsilon \ll 1$  we can proceed perturbatively by use of the expansion

$$\hat{\mathbf{u}} = [\hat{\mathbf{u}}_0(t) + \varepsilon \hat{\mathbf{u}}_1(t) + O(\varepsilon^2)] e^{\sigma t}$$

in (5.6). Averaging over one period leads to the condition that

$$\left\langle \frac{d}{dt} \left( \frac{1}{2} |\hat{\mathbf{u}}|^2 \right) \right\rangle = \varepsilon \tan \alpha \left[ \frac{\gamma + 1}{2} \right] \left\langle \cos \left( \frac{4}{\gamma} - 1 \right) t \right\rangle + O(\varepsilon^2).$$

Hence, for  $\varepsilon \rightarrow 0$ , growth occurs only at  $\gamma = 4$  or  $\cos \alpha = 1/4$  where

$$\sigma = \frac{2 \langle \hat{v}_0 \hat{w}_0 \rangle}{\langle \hat{\mathbf{u}}_0^2 \rangle} = \frac{5\sqrt{15}}{32} \approx 0.6052$$

to eliminate secularity in  $\hat{\mathbf{u}}_1$ .

As indicated previously, this Kelvin mode has a period of  $4\pi$  compared to the strain field which has period  $2\pi$  in the rotating frame. The instability is thus, in similarity with the elliptical instability, one of subharmonic parametric resonance to this order. However in contrast to the elliptical instability, no simple vortex-stretching picture emerges due to the modified frequency of excitation. No longer can the growing disturbance maintain a net time-averaged vorticity in the stretching direction, but rather the vorticity is alternately aligned and anti-aligned with the direction of shear. As a result no simple exponentially-growing spinover solution (Waleffe, 1990) of constant vorticity is available; any such disturbance possesses only algebraic growth at best.

The 'unbounded' analysis presented above is in effect an idealisation of a small scale disturbance evolving at the centre of a precessing spheroid. As such it may be expected to capture the most favoured form of disturbance free from constraining boundaries; as was the case for elliptical streamlines. This hypothesis is certainly not contradicted by the limited sampling of resonances presented in this paper, whose growth rates all respect the unbounded 'supremum' result of  $\bar{\sigma} = 5\sqrt{15}/32\varepsilon \approx 0.6052\varepsilon$ . Furthermore, the growth rates deduced by Mahalov (1992) for travelling waves in his infinite cylinder study are also all less than this figure.

## 6. DISCUSSION

We have seen that Poincaré's constant-vorticity solution for the motion within a precessing spheroid represents a globally strained, rotating flow. This straining field consists of two components; a boundary-induced elliptical part which acts in the plane of the streamlines, and a shearing part directed across the plane. Both components can parametrically resonate pairs of inertial waves with growth rates which scale with the magnitude of straining (i.e.  $\varepsilon$  and  $\beta$ ). The mechanism is inertial and local in the sense that, regardless of the scale, a patch of elliptical and/or sheared streamlines will breakdown to three-dimensional disturbances in the absence of viscous processes.

Confined within encircling boundaries, such disturbances could be expected to favour the central axis as a site for initial growth and this is certainly what is found for an elliptically-distorted spheroid (Kerswell, 1992). Cardin (1992) has indicated that such localisation can be seen in recent precessional experiments (Vanyo *et al.*, 1992). Any breakdown of the viscous cylindrical shear layer should presumably be localised away from this axis.

This paper has discussed the possibility of instability but only hinted at its probability. A mapping of some low-order elliptical (Kerswell, 1993b) and shearing resonances (Section 2) against the required geometry  $c$  suggests a good 'covering', bearing in mind that surrounding every resonance is a 'danger zone' proportional to the relevant strain parameter  $\beta$  or  $\varepsilon$ . Given the many opportunities for resonances within the infinite set of modes available, the probability appears high that for a specific container, some resonance is close by. Whether of course this resonance is observed depends on the fluid viscosity. A pair of inertial waves can only grow if their joint rate of excitation exceeds the geometric mean of their viscous decay rates. This may be seen by adding the viscous decay rates  $\nu$  for each wave to the amplitude equations (2.9),

$$\begin{aligned} [\bar{\sigma} - (\frac{1}{2} + \lambda_a) i + \nu_a] A_0 &= \varepsilon(1 - \lambda_b) I B_0, \\ [\bar{\sigma} + (\frac{1}{2} - \lambda_b) i + \nu_b] B_0 &= \varepsilon(1 + \lambda_a) I^* A_0. \end{aligned}$$

The modified expression for  $\bar{\sigma}$  is

$$\bar{\sigma} = \frac{1}{2}i(\lambda_a + \lambda_b) - \frac{1}{2}(\nu_a + \nu_b) + \sqrt{\frac{1}{4}(\nu_a + \nu_b)^2 + [\varepsilon^2(1 - \lambda_b)(1 + \lambda_a)|I|^2 - \nu_a \nu_b]},$$

at perfect tuning  $\lambda_b = \lambda_a + 1$  and instability occurs when

$$\varepsilon_{crit} |I| \sqrt{-\lambda_a \lambda_b} = \sqrt{\nu_a \nu_b}. \tag{6.1}$$

If then seems plausible that there should be a non-zero critical precession rate function  $\Omega_{crit}(c, E)$  ( $E$  is the Ekman number) which determines the point of bifurcation of Poincaré's solution for any container and fluid.

Application of the criticality expression (6.1) to Malkus' experiments produces some interesting results. Malkus observed a laminar flow when  $\Omega = 1$  rev/min,

$$\eta = 49/576; \mu = 0.31; \varepsilon = 1.2 \times 10^{-2}; \beta = 3.7 \times 10^{-3}; \sqrt{E} = 3.2 \times 10^{-3}$$

where  $E$  is the Ekman number of the flow. At these values, the shearing growth rate dominates the elliptical growth rate and may be estimated as  $\approx 0.6\varepsilon = 0.72 \times 10^{-2}$ . Taking the viscous decay rate for the lowest spinover wave, which corresponds to a change in the rotation axis of the fluid observed in the experiments, we have  $\nu = 2.62\sqrt{E} = 0.83 \times 10^{-2}$ ; the two values are close and of the right relative size for sub-criticality. If we use  $\Omega = 4/3$  rev/min at which Malkus observed a turbulent flow, the revised estimate for the shearing growth rate of  $0.6\varepsilon \approx 1.03 \times 10^{-2}$  now exceeds the viscous damping rate; although crude, these estimates are encouraging.

As a model of the Earth's outer core, the precession of a homogeneous, incompressible fluid within a spheroidal container is of course a drastic idealization. Not only does it neglect compressibility, stratification, Lorentz forces and the solid inner core, but the convecting nature of the outer core is completely ignored [of note here is the current work by Zhang (1993a, b) who considers the inertial wave problem coupled with convection]. Despite these obvious inadequacies, the study of inertial waves would seem a reasonable starting point to examine the responses of a rapidly rotating core, especially in light of recent reports (Melchior and Ducarme, 1986; Aldridge and Lumb, 1987; Crossley *et al.*, 1991). With these caveats, we discuss the possible implications of this paper to the Earth.

For Earth-like parameters, the shearing strain produced by precession can be estimated as

$$\varepsilon = |\Omega/\omega| \sin 23.5^\circ \approx 4 \times 10^{-8}$$

and the magnitude of a typical growth rate as  $\approx 0.6\varepsilon = 2.4 \times 10^{-8}$ . The viscosity of the outer core fluid remains one of the least constrained parameters in geophysics; estimates for the Ekman number  $E$  based on seismic inferences and assumptions of water-like viscosity values differ by 8 orders of magnitude. Adopting the latter leads to an Ekman number of  $10^{-15}$  and viscous decay rates of  $\nu = s\sqrt{E} = 3s \times 10^{-8}$  where  $s$  is a coefficient typically of  $O(1)$ . Thus at this range of core viscosity, the shearing growth rates are the same order as the damping rates. If they exceed the damping, we can expect breakdown of the Poincaré solution, perhaps to a hydromagnetic analogue of the fully turbulent state found in experiments. This said, the deeper issue remains whether Poincaré's solution is actually a relevant model of the convecting outer core's response to precession.

The picture painted throughout this work has been a linear one describing only the behaviour of small disturbances. Efforts are in progress to understand the evolution of a resonant pair of inertial waves excited within an elliptically-distorted cylinder (Waleffe, 1989; Malkus and Waleffe, 1991; Kerswell, 1992). This isolates the elliptical coupling operator in a more accessible geometry for which experimental results are available (Malkus, 1989).

### *Acknowledgements*

I am grateful to Dr Willem Malkus for sharing his experimental experiences and enthusiasm for this problem. I would also like to thank Dr Alar Toomre who indirectly stimulated this work.

### *References*

- Aldridge, K. D. and Lumb, L. I., "Inertial waves identified in the Earth's fluid outer core," *Nature* **325**, 421–423 (1987).  
 Aldridge, K. D. and Toomre, A., "Axisymmetric inertial oscillations of a fluid in a rotating spherical container," *J. Fluid Mech.* **37**, 307–323 (1969).  
 Backus, G. E., "Normal modes of small oscillation of an incompressible non-viscous fluid in a corotating rigid container," Preprint (1992).  
 Bayly, B. J., "Three dimensional instability of elliptical flow," *Phys. Rev. Lett.* **57**, 2160–2163 (1986).

- Bondi, H. and Lyttleton, R. A., "On the dynamical theory of the rotation of the Earth: the effect of precession on the motion of the liquid core," *Proc. Cam. Phil. Soc.* **49**, 498 (1953).
- Bryan, G. H., "The waves on a rotating liquid spheroid of finite ellipticity," *Phil. Trans. A* **180**, 187–219 (1989).
- Busse, F. H., "Steady fluid flow in a precessing spheroidal shell," *J. Fluid Mech.* **33**, 739–751 (1968).
- Cardin, P., private communication (1992).
- Cartan, M. E., "Sur les petites oscillations d'une masse fluide," *Bull. Sci. Math.* **46**, 317–352, 356–369 (1922).
- Chandrasekhar, S., *Ellipsoidal Figures of Equilibrium*, Yale University Press (1969); reprinted Dover, New York (1987).
- Craik, A. D. D., "The stability of unbounded two- and three-dimensional flows subject to body forces: some exact solutions," *J. Fluid Mech.* **198**, 275–292 (1989).
- Craik, A. D. D., "The stability of elliptical flows, unbounded and bounded," in: *Nonlinear Dynamics of Structures* conference proceedings, (Eds. Sagdeev, Frisch, Moiseev, Erokhin) (1991).
- Craik, A. D. D. and Allen, H. R., "The stability of three-dimensional time-periodic flows with spatially uniform strain rates," *J. Fluid Mech.* **234**, 613–627 (1992).
- Craik, A. D. D. and Criminale, W. O., "Evolution of wavelike disturbances in shear flows: a class of exact solutions of the Navier-Stokes equations," *Proc. Roy. Soc. Lond. A* **406**, 13–26 (1986).
- Crossley, D. J., Hinderer, J. and Legros, H., "On the excitation, detection and damping of core modes," *Phys. Earth Planet. Inter.* **68**, 97–116 (1991).
- Gans, R. F., "On the precession of a resonant cylinder," *J. Fluid Mech.* **41**, 865–872 (1970).
- Gledzer, E. B. and Ponomarev, V. M., "Instability of bounded flows with elliptical streamlines," *J. Fluid Mech.* **240**, 1–30 (1992).
- Gledzer, E. B., Novikov, Yu. V., Obukhov, A. M. and Chusov M. A., "An investigation of the stability of liquid flows in a three-axis ellipsoid," *Izv. Atmos. Ocean. Phys.* **10**, 69–71 (1974).
- Gledzer, E. B., Dolzhansky, F. V., Obukhov, A. M. and Ponomarev, V. M., "An experimental and theoretical study of the stability of motion of a liquid in an elliptical cylinder," *Izv. Atmos. Ocean. Phys.* **11**, 617–622 (1975).
- Greenspan, H. P., *The Theory of Rotating Fluids*, Cambridge University Press, Cambridge (1968); reprinted Breukelen Press, Brookline (1990).
- Hocking, L. M., "On the unsteady motion of a rotating fluid in a cavity," *Mathematika* **12**, 97–106 (1965).
- Johnson, L. E., "The precessing cylinder," in: *Notes on the 1967 Summer Study Program in Geophysical Fluid Dynamics at the Woods Hole Oceanographic Institute* Ref. 67–54, 85–108 (1967).
- Joseph, D. D., *Stability of Fluid Motions*, Springer-Verlag, New York (1976).
- Kerswell, R. R., "Elliptical instabilities of stratified, hydromagnetic waves and the Earth's outer core," Ph.D. Thesis M.I.T. (1992).
- Kerswell, R. R., "Elliptical instabilities of stratified, hydromagnetic waves," *Geophys. Astrophys. Fluid Dynam.* **71**, 105–143 (1993a).
- Kerswell, R. R., "Instabilities of tidally and precessionally induced flows," in: *Theory of Solar and Planetary Dynamos*. (Eds. M. R. E. Proctor, P. C. Matthews and A. M. Rucklidge). NATO ASI. Isaac Newton Lecture Note Series, pp. 181–188 (1993b).
- Kudlick, M. D., "On transient motions in a contained rotating fluid," Ph.D. Thesis, M.I.T. (1966).
- Lamb, H., *Hydrodynamics*, Cambridge University Press (1932); reprinted Dover, New York (1945).
- Lebovitz, N. R., "The stability equations for rotating, inviscid fluids: galerkin methods and orthogonal bases," *Geophys. Astrophys. Fluid Dynam.* **46**, 221–243 (1989a).
- Lebovitz, N. R., "Lagrangian perturbations of Riemann ellipsoids," *Geophys. Astrophys. Fluid Dynam.* **47**, 225–236 (1989b).
- Lyttleton, R. A., *The Stability of Rotating Liquid Masses*, Cambridge University Press (1953).
- Mahalov, A., "The instability of rotating fluid columns subjected to a weak external coriolis force," submitted to *Phys. Fluids* (1992).
- Malkus, W. V. R., "Precession of the Earth as the cause of geomagnetism" *Science* **169**, 259–264 (1968).
- Malkus, W. V. R., "An experimental study of global instabilities due to tidal (elliptical) distortion of a rotating elastic cylinder," *Geophys. Astrophys. Fluid Dynam.* **48**, 123–134 (1989).
- Malkus, W. V. R., "Energy sources for planetary dynamos," in: *Theory of Solar and Planetary Dynamos: Introductory Lectures*. (Eds. M. R. E. Proctor and A. D. Gilbert). NATO ASI. Isaac Newton Lecture Note Series (1993).



- Malkus, W. V. R. and Waleffe, F. A., "The transition from order to disorder in elliptical flow: a direct path to shear flow turbulence," in: *Advances in Turbulence 3* (Eds. A. V. Johansson and P. H. Alfredsson) Springer-Verlag Berlin, Heidelberg, 197–203 (1991).
- Manasseh, R., "Breakdown regimes of inertia waves in a precessing cylinder," *J. Fluid Mech.* **243**, 261–296 (1992).
- McEwan, A. D., "Inertial oscillations in a rotating fluid cylinder," *J. Fluid Mech.* **40**, 603–640 (1970).
- Melchior, P. and Ducarme, B., "Detection of inertial gravity oscillations in the Earth's core with a superconducting gravimeter at Brussels," *Phys. Earth Planet. Inter.* **42**, 129 (1986).
- Pierrehumbert, R. T., "Universal short-wave instability of 2-dimensional eddies in an inviscid fluid," *Phys. Rev. Lett.* **57**, 2157–2159 (1986).
- Poincaré, H., "Sur l'équilibre d'une masse fluide animée d'un mouvement de rotation," *Acta Math.* **7**, 259–380 (1885).
- Poincaré H., "Sur la précession des corps déformable," *Bull. Astron.* **27**, 321 (1910).
- Roberts, P. H. and Stewartson, K., "On the motion in a liquid in a spheroidal cavity of a precessing rigid body II," *Proc. Camb. Phil. Soc.* **61**, 279–288 (1965).
- Scott, W. E., "The frequency of inertial waves in a rotating, sectored cylinder," *J. Appl. Mech. Trans. ASME E*: **43**, 571–574 (1975).
- Stergiopoulos, S. and Aldridge, K. D., "Inertial waves in a fluid partially filling a cylindrical cavity during spin-up from rest," *Geophys. Astrophys. Fluid Dynam.* **21**, 89–112 (1982).
- Stewartson, K. and Roberts, P. H., "On the motion of a liquid in a spheroidal cavity of a precessing rigid body," *J. Fluid Mech.* **17**, 1–20 (1963).
- Thompson, R., "Diurnal tides and shear instabilities in a rotating cylinder," *J. Fluid Mech.* **40**, 737–751 (1970).
- Vanyo, J. P., "A geodynamo powered by luni-solar precession," *Geophys. Astrophys. Fluid Dynam.* **59**, 209–234 (1991).
- Vanyo, J. P., Wilde, P., Cardin, P. and Olson, P., "Flow structures induced in the liquid core by precession," abstract A.G.U. *EOS* **73**, 63 (Supplement) (1992).
- Vladimirov, V. A. and Tarasov, V., "Resonance instability of the flows with closed streamlines," in: *Laminar-Turbulent Transition: IUTAM Symposium Novosibirsk* (1984) (Ed. V. V. Kozlov) Springer Verlag, Berlin, Heidelberg, 717–722 (1985).
- Vladimirov, V. A. and Vostretsov, D., "Instability of steady flows with constant vorticity in vessels of elliptic cross-section," *Prikl. Matem. Mekhan.* **50**(3), 367–377 (1986) (Trans. in *J. Appl. Math. Mech.* **50**(3), 369–377).
- Vladimirov, V. A., Maharenko V. G. and Tarasov V. F., "Experimental investigation of non-axisymmetric inertial waves in a rotating fluid," *Izu. Akad. Nauk SSSR, Mekh. Zhidk i Gaza* **1**, 176–180, (1987) (Transl. in *Fluid Dynamics* **22**,1, 151–156).
- Waleffe, F. A., "The 3D instability of a strained vortex and its relation to turbulence," *Ph.D. Thesis, M.I.T.* (1989).
- Waleffe, F. A., "On the three-dimensional instability of a strained vortex," *Phys. Fluids A* **2**(1), 76–80 (1990).
- Whiting, R. D., "An experimental study of forced asymmetric oscillations in a rotating liquid filled cylinder," *Ballistic Research Labs. Rep. ARBRL-TR-02376* (1981).
- Zhang, K., "On equatorially trapped boundary inertial waves," *J. Fluid Mech.* **248**, 203–217 (1993a).
- Zhang, K., "Spherical inertial oscillation and convection," in: *Theory of Solar and Planetary Dynamos*. (Eds. M. R. E. Proctor, P. C. Matthews and A. M. Rucklidge). NATO ASI. Isaac Newton Lecture Note Series, pp. 339–346 (1993b).

## APPENDIX A

Here we prove the assertion made in Section 4 that if  $\mathbf{u}$  is a small disturbance riding upon Poincaré's basic solution whose time evolution is governed by (4.2) then

$$\mathbf{u}(\mathbf{x}, 0) \in \mathcal{V}_n \Rightarrow \mathbf{u}(\mathbf{x}, t) \in \mathcal{V}_n \quad \forall t > 0 \quad (\text{A.1})$$

where  $\mathcal{V}_n$  is the vector space spanned by  $\{\mathbf{Q}_{nmk}; -n \leq m \leq n; k = 1, \dots, k_{max}(n, m)\}$ . We start by arguing for the weaker result

$$\mathbf{u}(\mathbf{x}, 0) \in \bigoplus_{n=1}^N \mathcal{V}_n \Rightarrow \mathbf{u}(\mathbf{x}, t) \in \bigoplus_{n=1}^N \mathcal{V}_n \quad \forall t > 0. \tag{A.2}$$

The spatial component of a Poincaré modal pressure function is

$$\Phi_{nmk}(r, z) e^{im\phi} = r^{|m|} z^{\nu} e^{im\phi} \prod_1^N \left\{ \bar{x}_j^2 (\bar{x}_j^2 - 1) + \bar{x}_j^2 \left( \frac{r}{A_{nmk}} \right)^2 + (1 - \bar{x}_j^2) \left( \frac{z}{B_{nmk}} \right)^2 \right\}$$

i.e. a polynomial in  $x, y$  and  $z$  of degree  $n$  containing either all even or all odd degree terms. Consequently the components of  $\mathbf{Q}_{nmk}$  are polynomials of degree  $n - 1$  with lower order terms differing in degree from  $n - 1$  by 2. The set of all Poincaré modal velocities is commonly considered complete, that is, they are imagined to span the space of all incompressible velocities which satisfy the boundary conditions (see the recent proof by Backus, 1992). Therefore we may write the vector space of all such velocities of degree  $\leq N - 1$  as

$$\bigoplus_{n=1}^N \mathcal{V}_n.$$

In the precessing frame, the linearised Euler equation reads

$$\frac{\partial \mathbf{u}}{\partial t} + 2\boldsymbol{\Omega} \times \mathbf{u} + \mathbf{A} \cdot \mathbf{x} \cdot \nabla \mathbf{u} + \mathbf{A} \cdot \mathbf{u} + \nabla p = \mathbf{0} \tag{A.3}$$

where  $\mathbf{U} = \mathbf{A} \cdot \mathbf{x}$  is the basic state and the boundary condition is

$$xu_x + yu_y + \frac{z}{c^2} u_z = 0|_{\partial V}. \tag{A.4}$$

From these it is clear that if the components of  $\mathbf{u}$  are polynomials of degree  $N$  (and  $p$  of degree  $N + 1$ ) then  $\mathbf{u}$  will remain a polynomial of degree  $N$  for all subsequent times: this is statement (A.2). The two crucial ingredients for this result are firstly that the basic state is purely linear in the spatial coordinates. This ensures that each of the terms in (A.3) are polynomials of the same degree; and secondly that the boundary condition also possesses this property of homogeneity.

To arrive at the much stronger result (A.1), we define the operator  $\mathcal{F}$ ,

$$\mathcal{F}(\mathbf{u}) = -\mathbf{A} \cdot \mathbf{x} \cdot \nabla \mathbf{u} - \mathbf{A} \cdot \mathbf{u} - 2\boldsymbol{\Omega} \times \mathbf{u}, \tag{A.5}$$

which has the accompanying adjoint

$$\mathcal{F}^+(\mathbf{u}) = \mathbf{A} \cdot \mathbf{x} \cdot \nabla \mathbf{u} - \mathbf{A}^T \cdot \mathbf{u} - 2\boldsymbol{\Omega} \times \mathbf{u} \quad (\text{A.6})$$

under the inner product

$$\langle \mathbf{v}, \mathbf{u} \rangle = \iiint \mathbf{v}^+ \cdot \mathbf{u} \, dV.$$

The linearised Euler equation for a disturbance then can be written as

$$\frac{\partial \mathbf{u}}{\partial t} = \mathcal{F}(\mathbf{u}) - \nabla p \quad (\text{A.7})$$

and its dual

$$\frac{\partial \mathbf{u}}{\partial t} = \mathcal{F}^+(\mathbf{u}) - \nabla p. \quad (\text{A.8})$$

We now prove that  $\mathcal{V}_N$  is invariant under time evolution governed either by (A.7) or by its dual (A.8): put more succinctly

$$\mathcal{F} : \mathcal{V}_N \rightarrow \mathcal{V}_N \quad \text{and} \quad \mathcal{F}^+ : \mathcal{V}_N \rightarrow \mathcal{V}_N. \quad (\text{A.9})$$

Firstly (A.2) trivially implies (A.1) [or (A.9)] in the special cases  $N = 2$  and  $N = 3$ , because  $\mathcal{V}_1 = \{\mathbf{0}\}$  and only spaces differing by 2 can possibly be coupled by either (A.7) or (A.8). Now we proceed by induction. Assuming the result (A.9) holds for all  $n \leq N - 1$ , consider a disturbance  $\mathbf{u}(\mathbf{x}, t)$  which is such that  $\mathbf{u}(\mathbf{x}, 0) \in \mathcal{V}_N$ . Let  $\mathbf{v} = \mathbf{v}(\mathbf{x})$  be an arbitrary velocity field in

$$\bigoplus_{n=1}^{N-1} \mathcal{V}_n$$

so that  $\langle \mathbf{v}, \mathbf{u}(\mathbf{x}, 0) \rangle = 0$ . We can find how this overlap integral changes with time by taking the inner product of  $\mathbf{v}$  with (A.7). This gives

$$\frac{\partial}{\partial t} \langle \mathbf{v}, \mathbf{u} \rangle = \langle \mathbf{v}, \mathcal{F}(\mathbf{u}) \rangle$$

where the pressure term drops due to  $\mathbf{v}$  being incompressible and having a vanishing normal velocity component at the boundary. Rewriting in terms of the adjoint,

$$\frac{\partial}{\partial t} \langle \mathbf{v}, \mathbf{u} \rangle = \langle \mathcal{F}^+(\mathbf{v}), \mathbf{u} \rangle, \quad (\text{A.10})$$

we can now appeal to one half of our inductive assumption, namely

$$\mathcal{F}^+(\mathbf{v}) \in \bigoplus_{n=1}^{N-1} \mathcal{V}_n,$$

to conclude that

$$\frac{\partial}{\partial t} \langle \mathbf{v}, \mathbf{u}(\mathbf{x}, 0) \rangle = 0.$$

Further time differentiations of (A.10) show that all higher time derivatives of the inner product vanish at  $t = 0$  implying that the orthogonality condition is preserved over time. A similar train of thought suffices for the dual result.

The essential ingredients for this proof are that the possibly time-dependent basic flow is purely linear in the spatial coordinates, the boundary conditions have a polynomial structure and that the Poincaré modes satisfy them. This result will therefore hold more generally for any such basic flow in a spheroidal container, rotating or not. Although such exact polynomial solutions certainly exist in an ellipsoidal container, no simple normal modes exist to construct them as developed here, that is, we lose our physically-relevant bases vectors. Instead, a broader set of polynomial functions are then the only building blocks with which to work; see Lebovitz (1989a, b) for a general discussion of their generation and an application to Riemann ellipsoids.

## APPENDIX B

Here we quote the 8 equations which arise from substituting the eigensolution

$$\mathbf{u} = \sum_{i=1}^8 \alpha_i \mathbf{v}_i e^{\sigma t}$$

into the vorticity equation given by  $\nabla \times$  (4.2):

$$\begin{aligned} -\sigma(3 + 2\eta)\alpha_1 - \sigma(5 + 4\eta)\alpha_2 - (1 + 2\eta)\alpha_3 + (3 + 4\eta)\alpha_4 - (1 + \eta)(3 + 2\eta)\mu\alpha_7 \\ + (1 + \eta)(2 + \eta)\mu\alpha_8 = 0, \\ (1 + 2\eta)\alpha_1 + (3 + 4\eta)\alpha_2 - \sigma(3 + 2\eta)\alpha_3 + \sigma(5 + 4\eta)\alpha_4 + \mu(1 + \eta)(5 + 3\eta)\alpha_5 \\ + \mu(1 + \eta)(3 - \eta)\alpha_6 = 0, \end{aligned}$$

$$\begin{aligned}
& -\mu(5+4\eta)\alpha_3 + \mu(3+2\eta)\alpha_4 - \sigma(3+\eta)\alpha_5 - \sigma(5+\eta)\alpha_6 + (1-\eta)\alpha_7 - (3+\eta)\alpha_8 = 0, \\
& \mu(1+\eta)\alpha_3 + 3\mu(1+\eta)\alpha_4 - \sigma(3+\eta)\alpha_5 + \sigma(5+\eta)\alpha_6 + (3+\eta)\alpha_7 - (1-\eta)\alpha_8 = 0, \\
& \quad -3\sigma\alpha_1 + 5\sigma\alpha_2 + 5\alpha_3 + 3\alpha_4 - \mu\alpha_7 - \mu(2+3\eta)\alpha_8 = 0, \\
& \quad -5\alpha_1 + 3\alpha_2 - 3\sigma\alpha_3 - 5\sigma\alpha_4 - \mu(1+3\eta)\alpha_5 + \mu(3+7\eta)\alpha_6 = 0, \\
& -\mu(4+3\eta)\alpha_1 - \mu(2+\eta)\alpha_2 + 4\alpha_5 - 2(1+\eta)\alpha_6 + \sigma(2+\eta)\alpha_7 - \sigma\alpha_8 = 0, \\
& \quad 4\mu(1+\eta)\alpha_2 - 4\alpha_5 - 2(1+\eta)\alpha_6 - \sigma\alpha_7 + \sigma(2+\eta)\alpha_8 = 0.
\end{aligned} \tag{B.1}$$

This is a matrix eigenvalue problem for  $\sigma$  of the form

$$(\sigma\mathbf{B} - \mathbf{C}) \cdot \boldsymbol{\alpha} = \mathbf{0},$$

where  $\mathbf{B}$  and  $\mathbf{C}$  are the  $8 \times 8$  matrices defined through the system (B.1).

## APPENDIX C

In this appendix, we sketch the asymptotic situation in the fourth tongue of Figure 3 emanating from  $\eta = 0.678574$  when  $\Omega \rightarrow 0$ . Here  $\varepsilon^2 = O(\beta)$  and so the shearing operator affects the leading order elliptical resonance at its second order. As described in Section 3, we need only calculate  $\mathbf{v}_{12}$  and its matrix elements in the amplitude equations (3.3) and (3.4) to capture the leading order growth:  $\mathbf{v}_{11}$  and  $\mathbf{v}_{13}$  are responsible for frequency shifting only.

In the notation of Section 3  $\mathbf{Q}_a = \mathbf{Q}_{3,0,1}$ ,  $\mathbf{Q}_b = \mathbf{Q}_{3,2,1}$ ,  $m_a = 0$ ,  $m_b = 2$ ,  $\lambda_a = \lambda_{3,0,1} = -1.087378$ ,  $\lambda_b = \lambda_{3,2,1} = 0.912622$ ,  $\lambda_{3,1,1} = 1.673081$ ,  $\lambda_{3,1,2} = -0.178645$  at  $\eta = 0.678574$ . We define  $\lambda = \lambda_{3,2,1} - 1 = \lambda_{3,0,1} + 1$  so that

$$\mathbf{v}_{12} = \hat{\mathbf{v}}_{12} e^{i(\phi + \lambda t)}.$$

According to Appendix A,  $\mathbf{v}_{12} \in \mathcal{V}_3$ , and hence

$$\mathbf{v}_{12} \in \langle \mathbf{Q}_{3,1,k}; k = 1, 2 \rangle e^{i\lambda t}.$$

However, for our purposes we need the pressure as well which forces reducing (3.2) to an equation solely for this. Representing the right-hand side of (3.2) as

$$[f_r, f_\phi, f_z]^T e^{i(\phi + \lambda t)}$$

where

$$\begin{aligned}
 f_r &= A \left[ \frac{\lambda_{3,0,1} + 1}{\lambda_{3,0,1}} \right] \frac{\partial \Phi_{3,0,1}}{\partial z} + B \left[ \frac{\lambda_{3,2,1} - 1}{\lambda_{3,2,1}} \right] \frac{\partial \Phi_{3,2,1}}{\partial z}, \\
 f_\phi &= iA \left[ \frac{\lambda_{3,0,1} + 1}{\lambda_{3,0,1}} \right] \frac{\partial \Phi_{3,0,1}}{\partial z} - iB \left[ \frac{\lambda_{3,2,1} - 1}{\lambda_{3,2,1}} \right] \frac{\partial \Phi_{3,2,1}}{\partial z}, \\
 f_z &= A \left[ \frac{1 + \lambda_{3,0,1}}{2 + \lambda_{3,0,1}} \right] \frac{\partial \Phi_{3,0,1}}{\partial r} + B \left[ \frac{1 - \lambda_{3,2,1}}{2 - \lambda_{3,2,1}} \right] \left( \frac{\partial \Phi_{3,2,1}}{\partial r} + \frac{2}{r} \Phi_{3,2,1} \right),
 \end{aligned} \tag{C.1}$$

the problem for the pressure  $p(\mathbf{x}, t) = p_{12}(r, z)e^{i(\phi + \lambda t)}$  becomes

$$\begin{aligned}
 \frac{1}{r} \frac{\partial}{\partial r} \left( r \frac{\partial p_{12}}{\partial r} \right) - \frac{1}{r} p_{12} + \left( 1 - \frac{4}{\lambda^2} \right) \frac{\partial^2 p_{12}}{\partial z^2} &= \frac{1}{r} \frac{\partial}{\partial r} (r f_r) - \frac{2}{\lambda r} f_r - \frac{2i}{\lambda r} \frac{\partial}{\partial r} (r f_\phi) \\
 &+ \frac{i}{r} f_\phi + \left( 1 - \frac{4}{\lambda^2} \right) \frac{\partial f_z}{\partial z}
 \end{aligned} \tag{C.2}$$

with boundary condition

$$r \frac{\partial p_{12}}{\partial r} + \frac{2}{\lambda} p_{12} + \frac{z}{c^2} \left( 1 - \frac{4}{\lambda^2} \right) \frac{\partial p_{12}}{\partial z} = r \left( f_r - \frac{2i}{\lambda} f_\phi \right) + \frac{z}{c^2} \left( 1 - \frac{4}{\lambda^2} \right) f_z \Big|_{\partial V}. \tag{C.3}$$

We can find a solution for  $p_{12}(r, z)e^{i\phi}$  as a simple linear combination of  $\Phi_{3,1,1}(\mathbf{x})$  and  $\Phi_{3,1,2}(\mathbf{x})$ . Then  $\mathbf{v}_{12}$  is retrieved via the relations

$$\begin{aligned}
 u_{12} &= \frac{1}{4 - \lambda^2} \left( -i\lambda \frac{\partial p_{12}}{\partial r} - \frac{2i}{r} p_{12} + i\lambda f_r + 2f_\phi \right), \\
 v_{12} &= \frac{1}{4 - \lambda^2} \left( 2 \frac{\partial p_{12}}{\partial r} + \frac{\lambda}{r} p_{12} + i\lambda f_\phi - 2f_r \right), \\
 w_{12} &= \frac{1}{i\lambda} \left( f_z - \frac{\partial p_{12}}{\partial z} \right).
 \end{aligned} \tag{C.4}$$

We are now in a position to calculate the matrix elements present in the coupled system (3.3)–(3.4):

$$\langle \mathbf{Q}_{3,0,1}, e^{-2i(\phi+t)} \mathcal{L}_E^+ (\mathbf{Q}_{3,2,1}, p_{3,2,1}) \rangle = \frac{i}{(2 + \lambda_{3,0,1})} \left( \frac{1}{2} \beta + \left[ \frac{1 - \lambda_{3,2,1}}{2 - \lambda_{3,2,1}} \right] \varepsilon^2 \right) J$$

and

$$\langle \mathbf{Q}_{3,2,1}, e^{2i(\phi+t)} \mathcal{L}_E(\mathbf{Q}_{3,0,1}, p_{3,0,1}) \rangle = \frac{-i}{(2 - \lambda_{3,2,1})} \left( \frac{1}{2} \beta + \left[ \frac{1 + \lambda_{3,0,1}}{2 + \lambda_{3,0,1}} \right] \varepsilon^2 \right) J$$

where

$$J = \iiint \frac{\partial \Phi_{3,0,1}}{\partial r} \left( \frac{\partial \Phi_{3,2,1}}{\partial r} + \frac{2}{r} \Phi_{3,2,1} \right) dV,$$

$$\langle \mathbf{Q}_{3,0,1}, e^{-i(\phi+t)} \mathcal{L}_S^+(\mathbf{v}_{12}, p_{12}) \rangle = \langle \mathbf{Q}_{3,0,1}, \left[ \begin{array}{c} \left( \frac{\lambda - 1}{\lambda} \right) \frac{\partial p_{12}}{\partial z} + \frac{f_z}{\lambda} \\ -i \left( \frac{\lambda - 1}{\lambda} \right) \frac{\partial p_{12}}{\partial z} - \frac{if_z}{\lambda} \\ \left( \frac{1 - \lambda}{2 - \lambda} \right) \left( \frac{\partial p_{12}}{\partial r} + \frac{1}{r} p_{12} \right) \end{array} \right] \rangle,$$

$$\langle \mathbf{Q}_{3,2,1}, e^{i(\phi+t)} \mathcal{L}_S(\mathbf{v}_{12}, p_{12}) \rangle = \langle \mathbf{Q}_{3,2,1}, \left[ \begin{array}{c} \left( \frac{\lambda + 1}{\lambda} \right) \frac{\partial p_{12}}{\partial z} - \frac{f_z}{\lambda} \\ i \left( \frac{\lambda + 1}{\lambda} \right) \frac{\partial p_{12}}{\partial z} - \frac{if_z}{\lambda} \\ \left( \frac{1 + \lambda}{2 + \lambda} \right) \left( \frac{\partial p_{12}}{\partial r} - \frac{1}{r} p_{12} \right) \end{array} \right] \rangle.$$

Putting it all together produces a growth rate of  $0.630487\beta$ , coinciding exactly with the numerical result.